Supplementary Information for

Dimeric palladium 1,2,3-triazol-5-ylidene complexes – synthesis, structure, reactivity and catalytic properties in Suzuki coupling

Jan Lorkowski, Patrycja Żak, Maciej Kubicki, Cezary Pietraszuk,* Dawid Jędrzkiewicz, Jolanta Ejfler*

Submitted to New Journal of Chemistry

Table of Content

1. Synthesis and characterization of triazoles

*Synthesis of 1-(2,4,6-trimethylphenyl)-4-phenyl-1H-1,2,3-triazole (**1a**).*

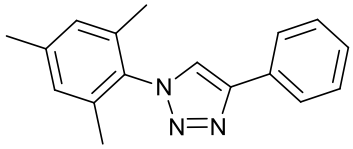

Triazole **1a** was prepared by previously reported protocol[S1]. 2,4,6-trimethylaniline (1 g, 7.4 mmol) was dissolved in acetonitrile (5 mL) in a 25 mL round bottomed flask equipped with a magnetic stirring bar. Mixture was cooled to 0 °C in the ice bath and *t*-BuONO (1.15 g, 11.1 mmol, 1.5 equiv) and Me_3SiN_3 (1.05 g, 7.4 mmol, 1 equiv) were sequentially added. The reaction mixture was stirred for 2 hours without removing a cooling bath. Then, sodium ascorbate (0.75 g, 3.7 mmol, 0.5 equiv), $CuSO_4x5H_2O$ (0.19 g, 0.74 mmol, 0.1 equiv) and phenylacetylene (1.15 g, 11.1 mmol, 1.5 equiv) in water (5 mL) were added. The reaction mixture was allowed to slowly warm up to room temperature while stirring overnight. The reaction mixture was quenched by adding an excess of conc. aq. ammonia and the resulting mixture was stirred for 12 h. The product was extracted with dichloromethane (3 × 10 mL) and the combined organic fractions were dried over anhydrous $MgSO_4$. After evaporation of the solvent, the crude product was washed with hexane (3×20 mL), to yield **1a** as a white solid (1.63 g, 84%). ^{1}H NMR (300 MHz, $CDCl_3$, ppm) δ 7.93 (d, *J* = 7.0 Hz, 1H), 7.84 (s, 1H), 7.49-7.44 (m, 2H), 7.39-7.34 (m, 1H) 7.01 (s, 2H), 2.37 (s, 3H), 2.02 (s, 6H). ^{13}C NMR (75 MHz, $CDCl_3$) δ 147.7, 140.2, 135.2, 133.6, 130.6, 129.2, 129.0, 128.4, 125.8, 121.6, 21.2, 17.4. These NMR data matched those reported in the literature[S2]

*General procedure for the synthesis of triazoles **1b** and **1c***

Triazoles **1b** and **1c** were prepared by previously reported protocol.[S3] Two neck round bottomed flask equipped with a magnetic stirring bar and a condenser was charged with 1-Bromoalkane (11 mmol, 1.1 equiv), sodium azide (12 mmol, 1.2 equiv) and DMF/H_2O (4:1, 30 mL) and was heated at 95 °C overnight. After cooling down, phenylacetylene (10 mmol, 1 equiv), sodium ascorbate (10 mmol, 1 equiv) and $CuSO_4{\cdot}5H_2O$ (2 mmol, 0.2 equiv) were added and the resulting mixture was stirred for another 48 h. The solution was added to the solution of EDTA 0.5 g in aq. ammonia (200 mL) and stirred for a further 1 h. The white solid was filtered and washed with water (3 × 200 mL), dissolved in dichloromethane (100 mL) and washed with water (3×100 mL) and brine (3 × 100 mL) and dried over anhydrous $MgSO_4$. After evaporation of the solvent, crude product was purified by column chromatography (dichloromethane → 9:1 dichloromethane /acetone, v/v) to give desired products.

1-hexyl-4-phenyl-1*H*-1,2,3-triazole (**1b**)

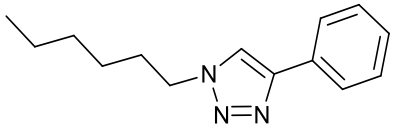

White solid**,** yield 79%, ^{1}H NMR (400 MHz, $CDCl_3$) δ: 7.83 (d, *J* = 7.1 Hz, 1H), 7.74 (s, 1H), 7.42 (t, *J* = 7.5 Hz, 1H), 7.38 – 7.29 (m, 1H), 4.40 (t, *J* = 7.2 Hz, 2H) 1.95 (m, 2H), 1.40 (m, 6H), 0.98 (t, *J* = 7.4 Hz,

3H). ^{13}C NMR (101 MHz, $CDCl_3$) δ 147.8, 130.8, 128.9, 128.2, 125.8, 119.4, 50.5, 31.3, 30.4, 26.3, 22.5, 14.1. These NMR data matched those reported in the literature[S3]

1-butyl-4-phenyl-1*H*-1,2,3-triazole (**1c**)

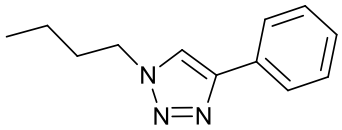

White solid, yield 84% ^{1}H NMR (300 MHz, $CDCl_3$) δ 7.86 – 7.81 (m, 2H), 7.74 (s, 1H) 7.46 – 7.38 (m, 2H), 7.36 – 7.29 (m, 1H), 4.40 (t, *J* = 7.2 Hz, 2H), 1.93 (m, 2H), 1.40 (m, 2H), 0.97 (t, *J* = 7.4 Hz, 3H).^{13}C NMR (75 MHz, $CDCl_3$) δ 147.8, 130.8, 128.9, 128.2, 125.8, 119.4, 50.2, 32.4, 19.8, 13.6. These NMR data matched those reported in the literature.[S4]

2. Synthesis and characterization of triazolium iodides

Triazolium Iodides **2 a-c** were prepared by previously reported protocol.[S5] 100 mL Schlenk tube equipped with a stirring bar and Rotaflo stopcock was charges with triazole (4.5 mmol), acetonitrile (8 mL) and methyl iodide (3.86 g, 27.2 mmol, 6 equiv). Reaction mixture was then stirred for 48 h at 80 °C. Solvent was removed under vacuum and then ethyl acetate (20 mL) was added to the solid residue. After stirring for 30 minutes white solid was filtered off and washed with ethyl acetate (3 × 20 mL). Remaining solid was dried under vacuum to give desired products.

1-mesityl-3-methyl-4-phenyl-1*H*-1,2,3-triazolium iodide (**2a**)

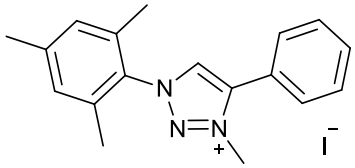

White solid, yield 71% ^{1}H NMR (400 MHz, $CDCl_3$) δ: 8.88 (s, 1H), 8.04 (d, *J* = 8.0 Hz, 2H), 7.63–7.55 (m, 3H), 7.04 (s, 2H), 4.58 (s, 3H), 2.37 (s, 3H), 2.22 (s, 6H). ^{13}C NMR (101 MHz, $CDCl_3$) δ 144.3, 142.6, 134.5, 132.2, 131.2, 130.5, 130.3, 130.1, 129.8, 121.4, 40.9, 21.37, 18.7. These NMR data matched those reported in the literature.[S6]

1-hexyl-3-methyl-4-phenyl-1*H*-1,2,3-triazolium iodide (**2b**)

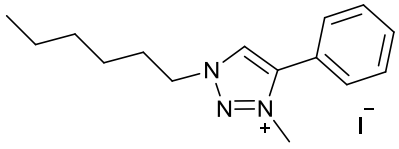

White solid, yield 74% ^{1}H NMR (400 MHz, $CDCl_3$) δ: 9.51 (s, 1H), 7.74 (d, *J* = 9.6 Hz, 2H), 7.60–7.51 (m, 3H), 4.77 (t, *J* = 7.2 Hz, 2H), 4.31 (s, 3H), 2.11-2.03 (m, 2H), 1.45 – 1.35 (m, 2H), 1.34–1.25 (m, 4H),

0.86 (t, J = 7.1 Hz, 3H). ^{13}C NMR (100 MHz, $CDCl_3$) δ 142.8, 131.8, 129.6, 129.6, 129.5, 121.6, 54.4, 39.2, 30.8, 29.3, 25.7, 22.2, 13.8. These NMR data matched those reported in the literature.[S7]

1-butyl-3-methyl-4-phenyl-1*H*-1,2,3-triazolium iodide (**2c**)

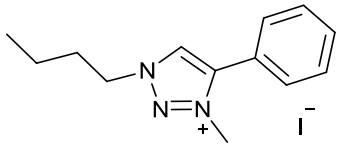

White solid, 67%, ^{1}H NMR (400 MHz, $CDCl_3$) δ: 9.52 (s, 1H), 7.72-7.70 (m, 2H), 7.61– 7.52 (m, 3H), 4.79 (t, J = 7.4 Hz, 2H), 4.31 (s, 3H), 2.06 (quint, J = 7.5 Hz, 2H), 1.44 (sex, J = 7.5 Hz, 2H), 0.96 (t, J = 7.4 Hz, 3H).^{13}C NMR (100 MHz, $CDCl_3$) δ 143.0, 132.1, 129.8, 129.8, 121.8, 54.4, 39.4, 31.4, 19.6, 13.5. These NMR data matched those reported in the literature.[S4]

3. X-ray crystallography

Diffraction data were collected by the ω-scan technique, for **3a (cisoid)** at 220(1) K, for **3c** at room temperature on Rigaku Xcalibur four-circle diffractometer with Eos CCD detector and graphite-monochromated MoK_α radiation (λ=0.71069 Å), for **3b** at 130(1) and for **3a(transoid)** at room temperature on Rigaku SuperNova four-circle diffractometer with Atlas CCD detector and mirror-monochromated CuK_α radiation (λ=1.54178 Å). The data were corrected for Lorentz-polarization as well as for absorption effects.[S8] Precise unit-cell parameters were determined by a least-squares fit of reflections of the highest intensity (5063 for **3a(cisoid)**, 6628 for **3a(transoid)**, 3168 for **3c**, 3548 for **3b**), chosen from the whole experiment. The structures were solved with SHELXT [2] and refined with the full-matrix least-squares procedure on F^2 by SHELXL-2013.[S9] All non-hydrogen atoms were refined anisotropically, hydrogen atoms were placed in idealized positions and refined as 'riding model' with isotropic displacement parameters set at 1.2 (1.5 for methyl groups) times U_{eq} of appropriate carrier atoms. In the crystal structure of **3a(cisoid)**, there are three solvent CH_2Cl_2 molecules of which two are heavily disordered. The diffraction data were collected at different temperatures, as it turned out that the samples decompose slowly during dat collection. Additionally, lowering temperature below 200K seemed to start additional changes in the crystal structure (twinning or phase transition), which caused additional effects. Therefore we decided to use the best (in our opinion) data we have, collected at 220K, and leave the analysis of the thermal behaviour of these crystals for additional investigation. The two out of three solvent molecules were disordered, the s.o.f.s were set at 0.75/0.25 and 0.85/0.15 on the basis of similar displacement parameters. The geometries of the disordered molecules were restrained to be similar to the single ordere solvent molecule, moreover, the less-occupied alternatives went unstable so they were fixed during last cycles of refinement.

Crystallographic data for the structural analysis has been deposited with the Cambridge Crystallographic Data Centre, Nos. CCDC-1842072 (**3a**-cisoidal), CCDC-1814491 (**3a**-*transoidal*) CCDC-1525786 (**3c**), and CCDC-1525787 (**3b**). Copies of this information may be obtained free of charge from: The Director, CCDC, 12 Union Road, Cambridge, CB2 1EZ, UK. Fax: +44(1223)336-033, e-mail:deposit@ccdc.cam.ac.uk, or www: www.ccdc.cam.ac.uk.

Table S1. Crystal data, data collection and structure refinement

Compound	**3a** (cisoidal)	**3a** (transoidal)	**3b**	**3c**
Formula	$C_{36}H_{38}Cl_4N_6Pd_2 \cdot 3(CH_2Cl_2)$	$C_{36}H_{38}Cl_4N_6Pd_2 \cdot 1/4 H_2O$	$C_{30}H_{42}Cl_4N_6Pd_2$	$C_{26}H_{34}Cl_4N_6Pd_2 \cdot 2(CH_2Cl_2)$
Formula weight	1164.10	913.83	841.29	955.04
T(K)	220	295	130	295
λ(Å)	0.71069	1.54178	1.54178	0.71069
Crystal system	monoclinic	orthorhombic	triclinic	triclinic
Space group	$P2_1/n$	Pcca	P-1	P-1
a(Å)	11.7859(14)	19.2313(4)	8.5086(5)	9.6142(6)
b(Å)	17.1438(16)	9.34530(16)	9.6382(7)	9.6671(7)
c(Å)	23.6237(17)	21.9179(5)	11.0676(9)	10.4555(8)
α(°)	90	90	87.990(6)	94.150(6)
β(º)	90.536(3)	90	85.619(6)	91.958(6)
γ(°)	90	90	74.108(6)	108.730(6)
V($Å^3$)	4773.1(8)	3939.14(14)	870.29(11)	916.18(12)
Z	4	4	1	1
D_x(g cm^{-3})	1.62	1.54	1.61	1.73
F(000)	2328	1834	424	476
μ(mm^{-1})	1.35	10.13	11.39	1.59
Θ range (^{0})	2.87 – 25.00	4.03 – 67.5	4.01 – 75.39	3.64 – 26.46
Reflections:				
collected	34672	28475	5824	6312
unique (R_{int})	8389 (0.089)	3558 (0.035)	3473 (0.031)	3491 (0.018)
with I>2σ(I)	3748	3289	3316	3235
R(F) [I>2σ(I)]	0.084	0.029	0.063	0.027
$wR(F^2)$ [I>2σ(I)]	0.188	0.075	0.154	0.062
R(F) [all data]	0.190	0.033	0.064	0.029
$wR(F^2)$ [all data]	0.227	0.076	0.155	0.064
Goodness of fit	0.98	1.11	1.16	1.07
max/min Δρ (e $Å^{-3}$)	1.03/-0.64	0.53/-0.44	2.91/-1.40	1.74/-0.86
CCDC number	1842072	1814491	1525786	1525787

Table S2. Selected geometrical data (Å,º) with s.u.'s in parentheses

	3a (cisoidal)	**3a** (transoidal)	**3b**	**3c**
Pd-C	1.951(10) 1.928(10)	1.955(3)	1.954(6)	1.948(3)
Pd-Cl(b)	2.352(3) 2.421(3) 2.337(3) 2.422(3)	2.3141(8) 2.4228(7)	2.3217(14) 2.411(14)	2.3272(7) 2.4063(7)
Pd-Cl(t)	2.301(3) 2.305(3)	2.2646(10)	2.3078(14)	2.2943(7)
Pd···Pd	3.4537(12)	3.2468(4)	3.256	3.264
C-Pd-Cl(b)	173.5(3) 173.0(3)	178.08(9)	175.23(8)	177.86(5)
Cl(b)-Pd-Cl(t)	178.50(10) 177.63(10)	177.10(8)	178.30(3)	177.04(16)
Pd-Cl-Pd	94.89(10) 90.99(9)	86.51(2)	92.84(2)	93.10(5)
N1-C5-C4	101.7(9) 101.5(9)	104.4(3)	104.1(2)	104.2(5)
N1-C5-Pd	128.0(8) 131.8(8)	127.3(2)	125.9(2)	127.4(4)
C4-C5-Pd	129.3(8) 126.5(8)	128.2(8)	129.6(2)	128.4(4)
Cl(t)-Pd···Pd-Cl(t)	4.8	146.2	180	180
A/B	61.9(3) 55.6(3)	52.6(10)	48.37(11)	50.4(3)
A/PdCCl$_3$	64.8(3) 79.8(3)	76.38(10)	81.92(7)	69.04(16)

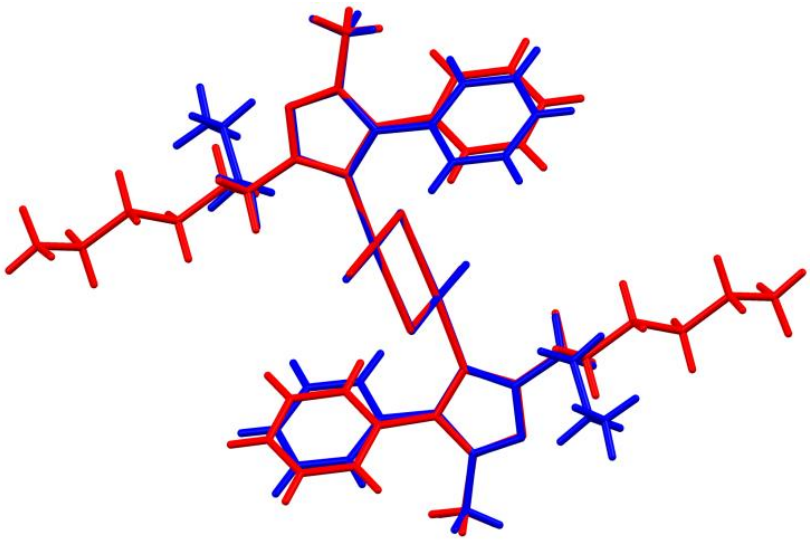

Figure S1. A comparison of the complexes from structures **3b** and **3c**.

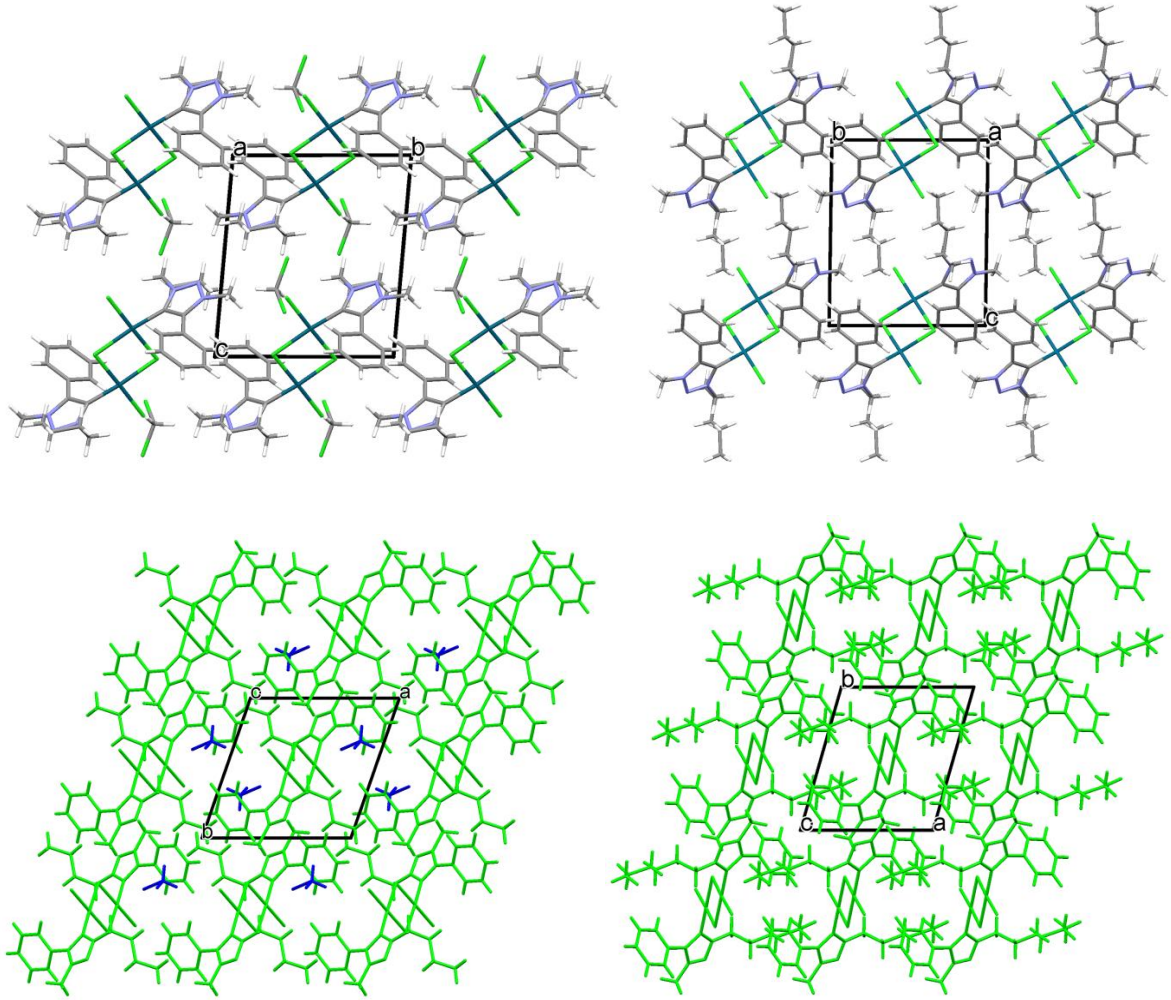

Figure S2. A comparison of crystal packing of complexes **3c** (left) and **3b** (right), as seen along x (upper row) and z (lower row) directions.

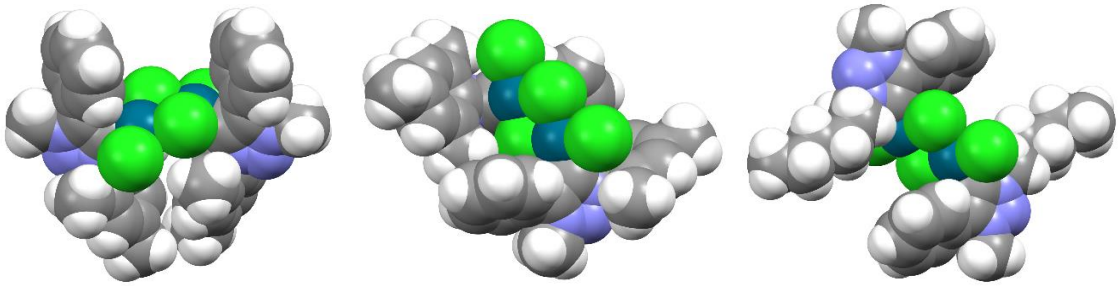

Figure S3. Van der Waals representation of complexes, from left to right **3a** (transoidal), **3a** (cisoidal) and **3b**.

4. NMR spectroscopic study of 3a-c in solution

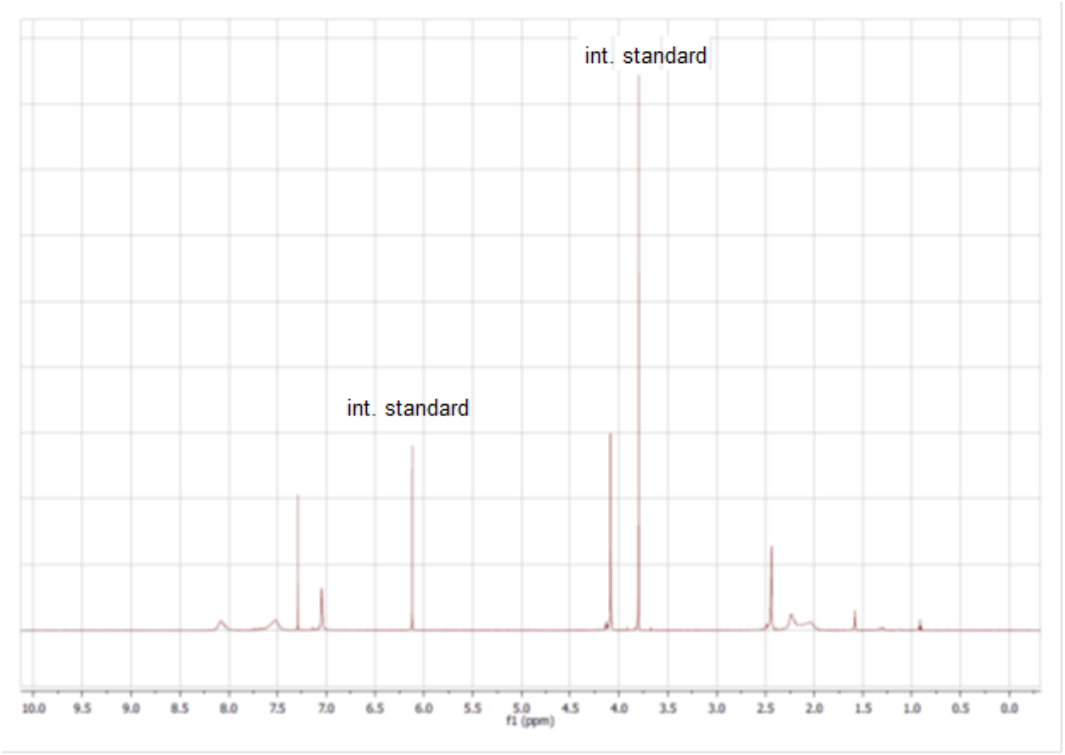

Figure S4. ^{1}H NMR spectrum of **3a** in $CDCl_3$ recorded at 298 K.
Int. standard = 1,2,3-trimethoxybenzene.

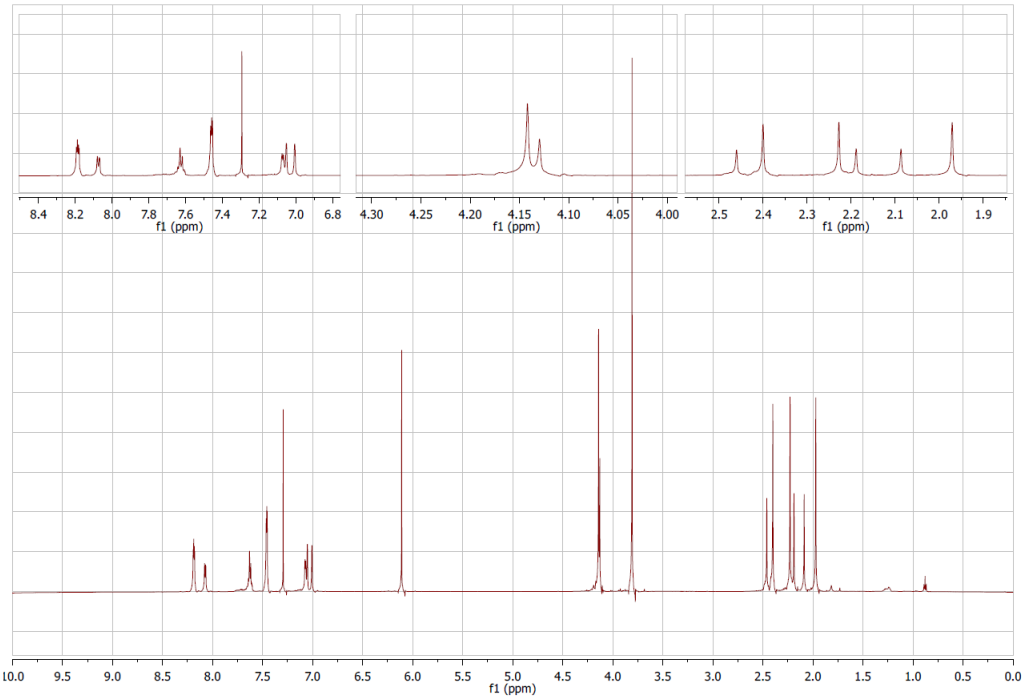

Figure S5. ^{1}H NMR spectrum of **3a** recorded at 225 K.

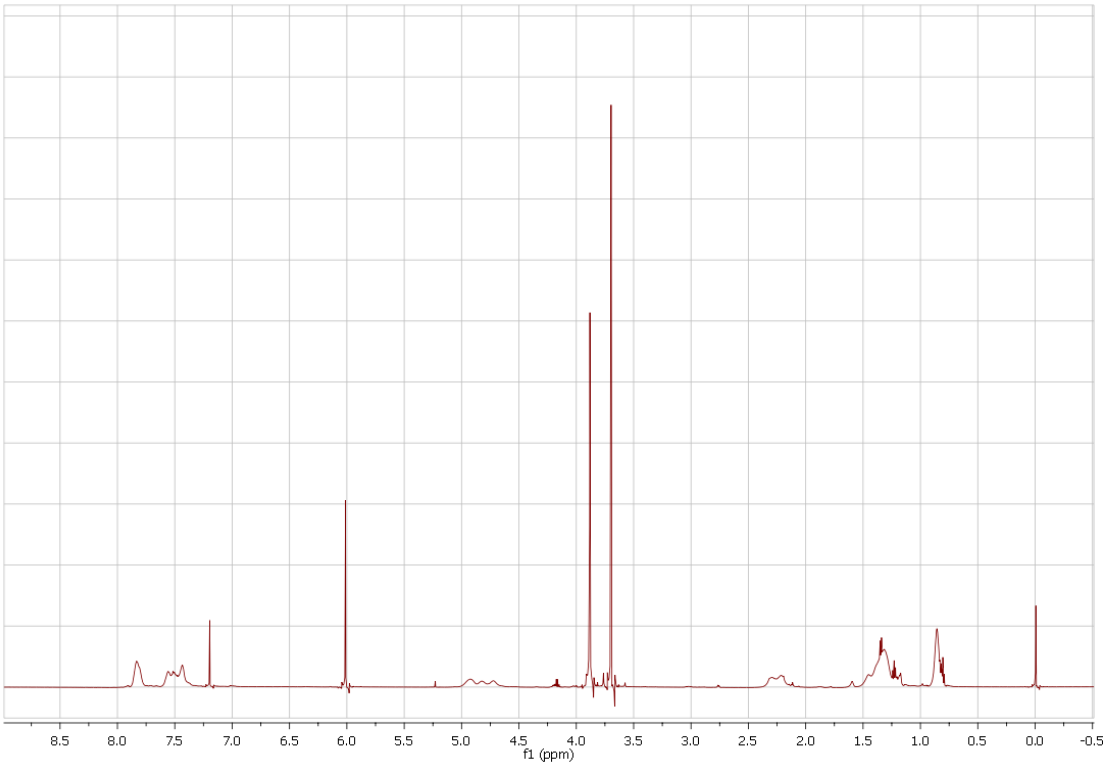

Figure S6. ^{1}H NMR spectrum of **3b** in $CDCl_3$ recorded at 298 K.

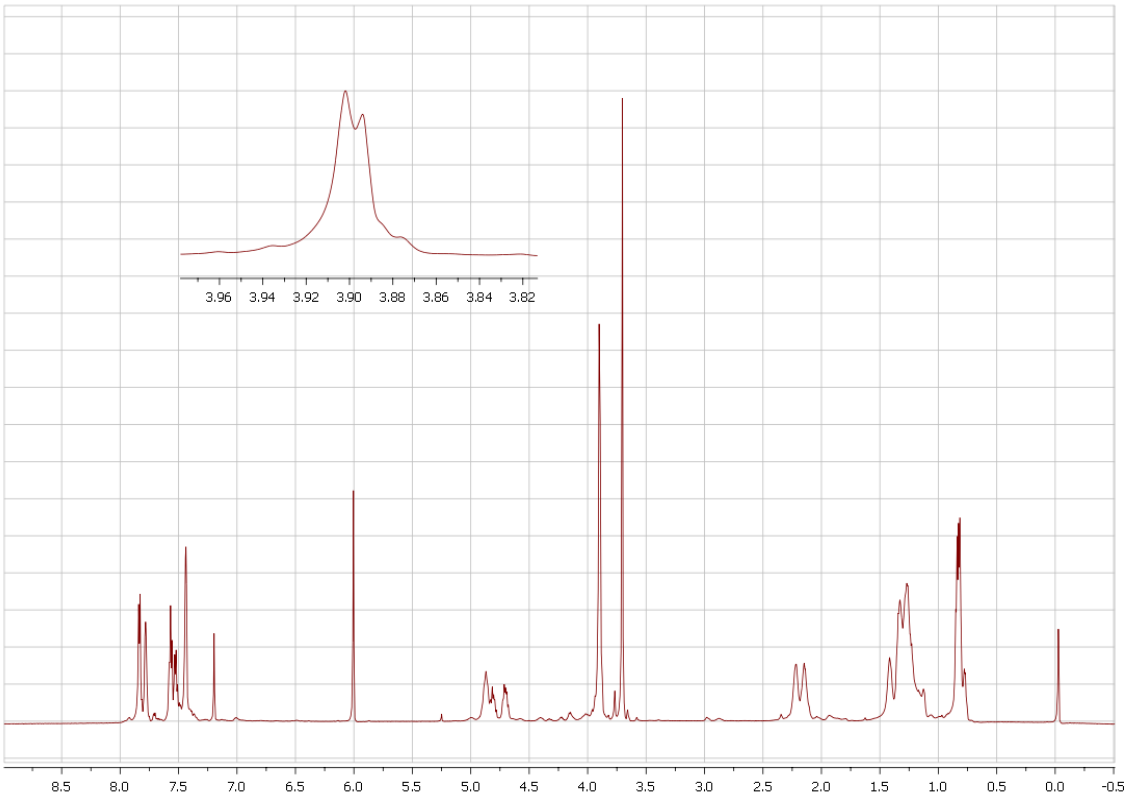

Figure S7. ^{1}H NMR spectrum of **3b** in $CDCl_3$ recorded at 216 K.

NMR spectra of complexes 3a-c

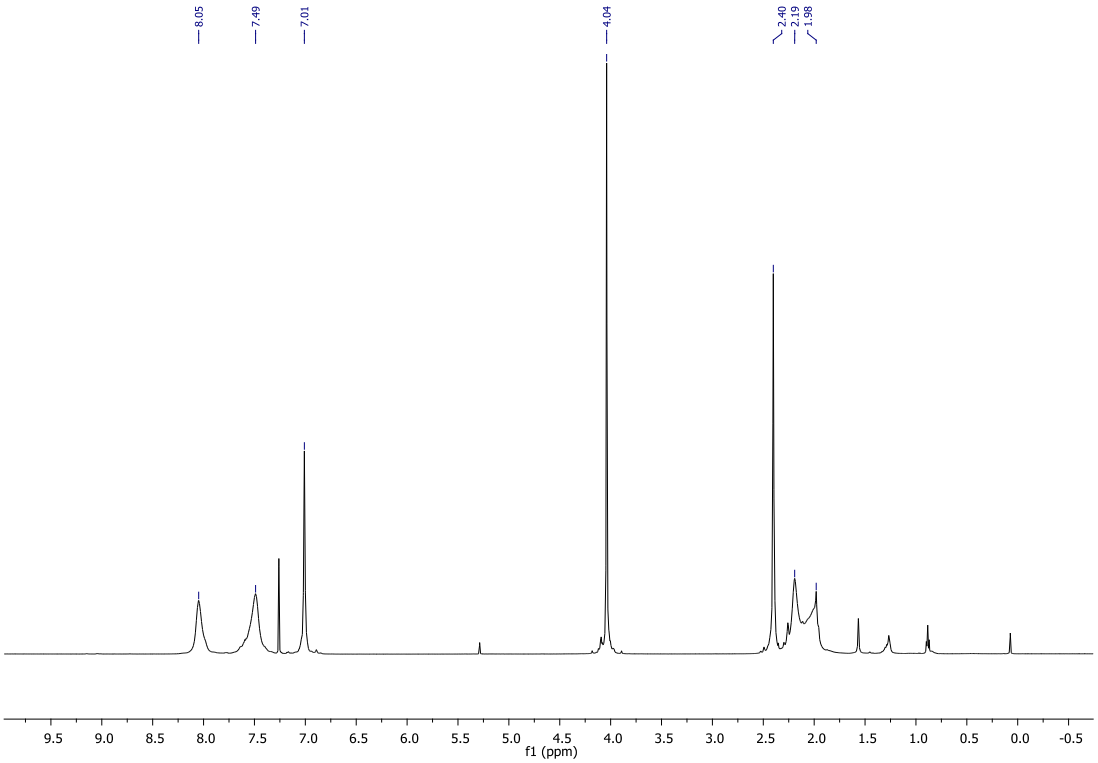

Figure S8. ^{1}H NMR spectra of **3a**

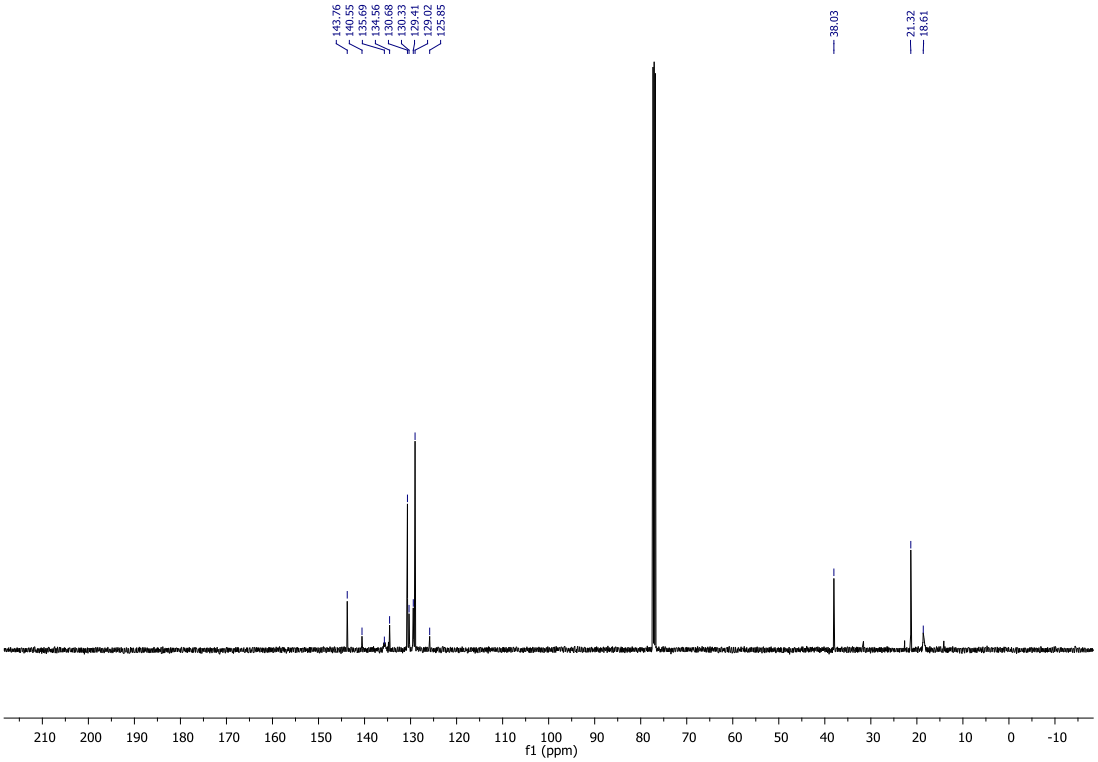

Figure S9. ^{13}C NMR spectra of **3a**

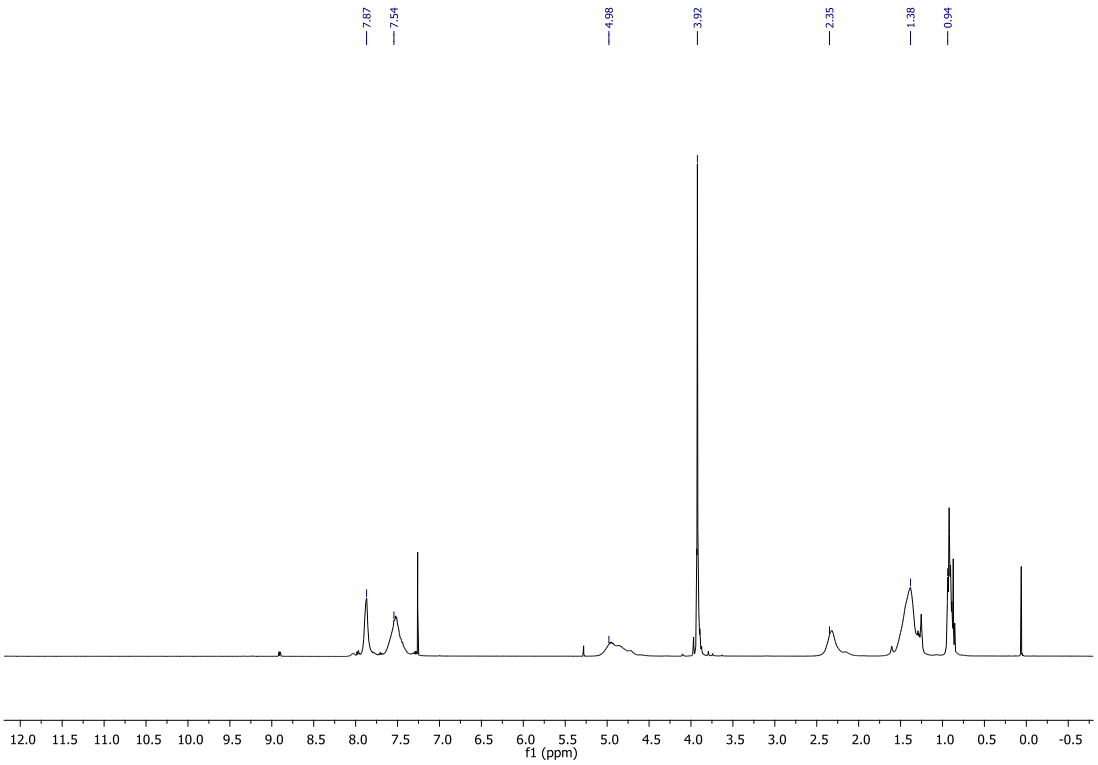

Figure S10. ^{1}H NMR spectra of **3b**

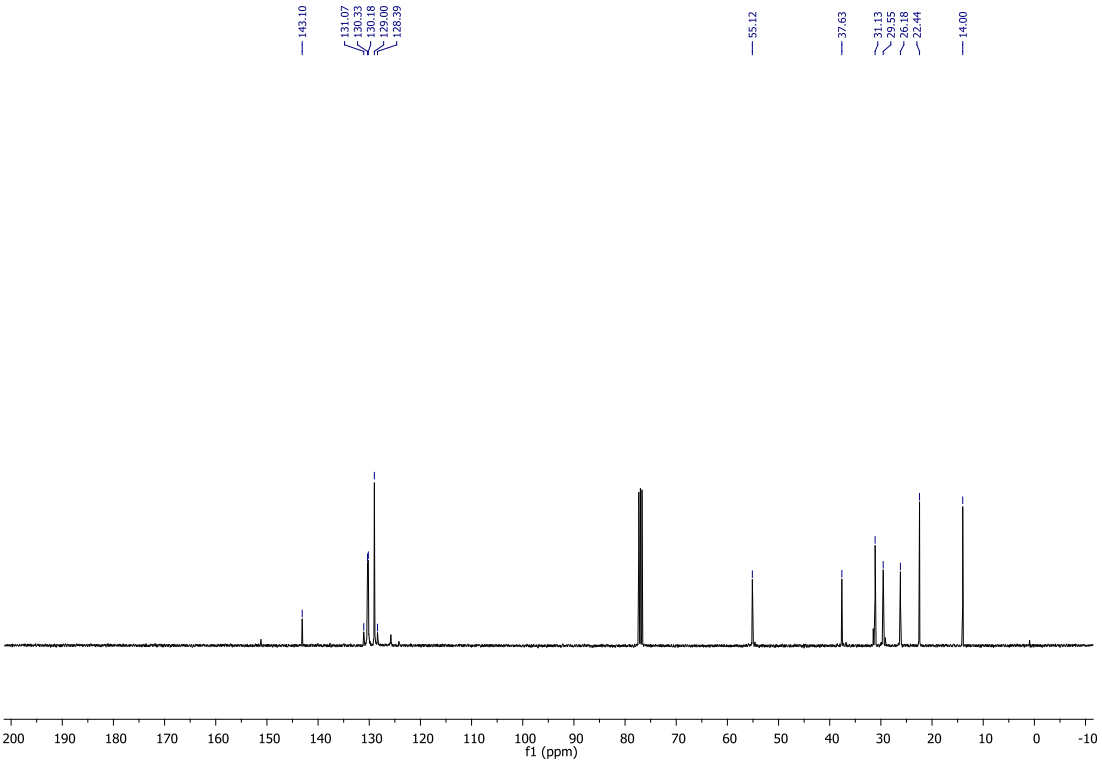

Figure S11. ^{13}C NMR spectra of **3b**

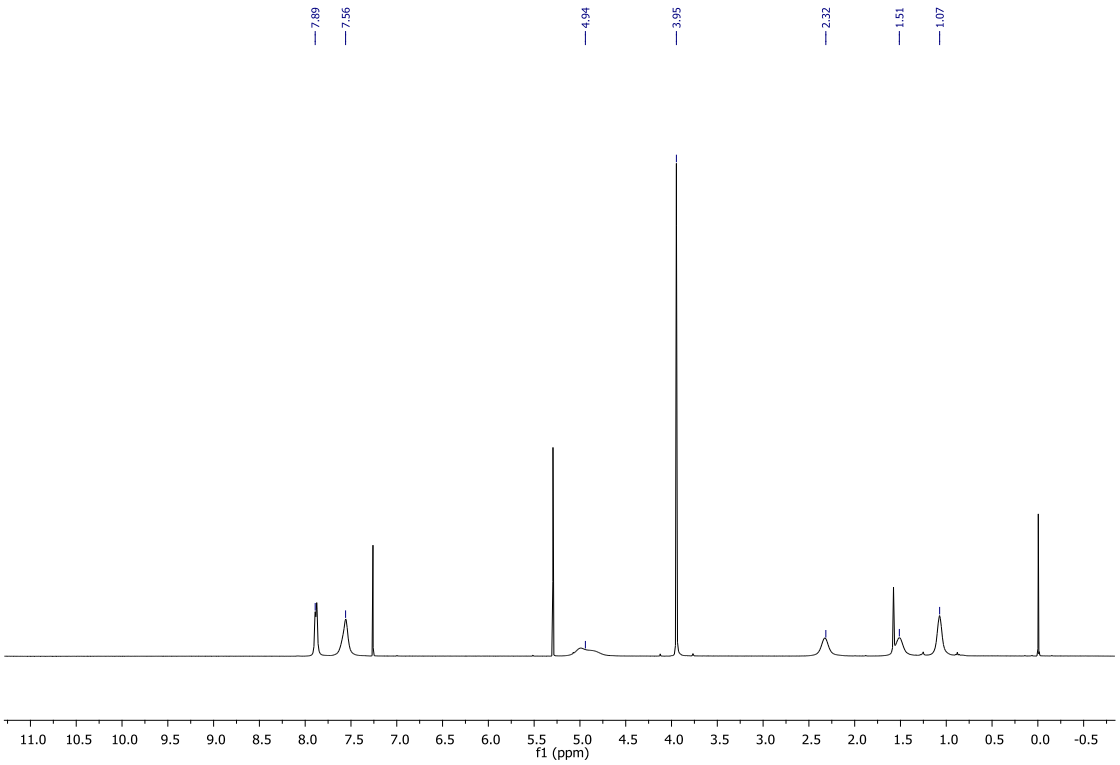

Figure S12. ^{1}H NMR spectra of **3c**

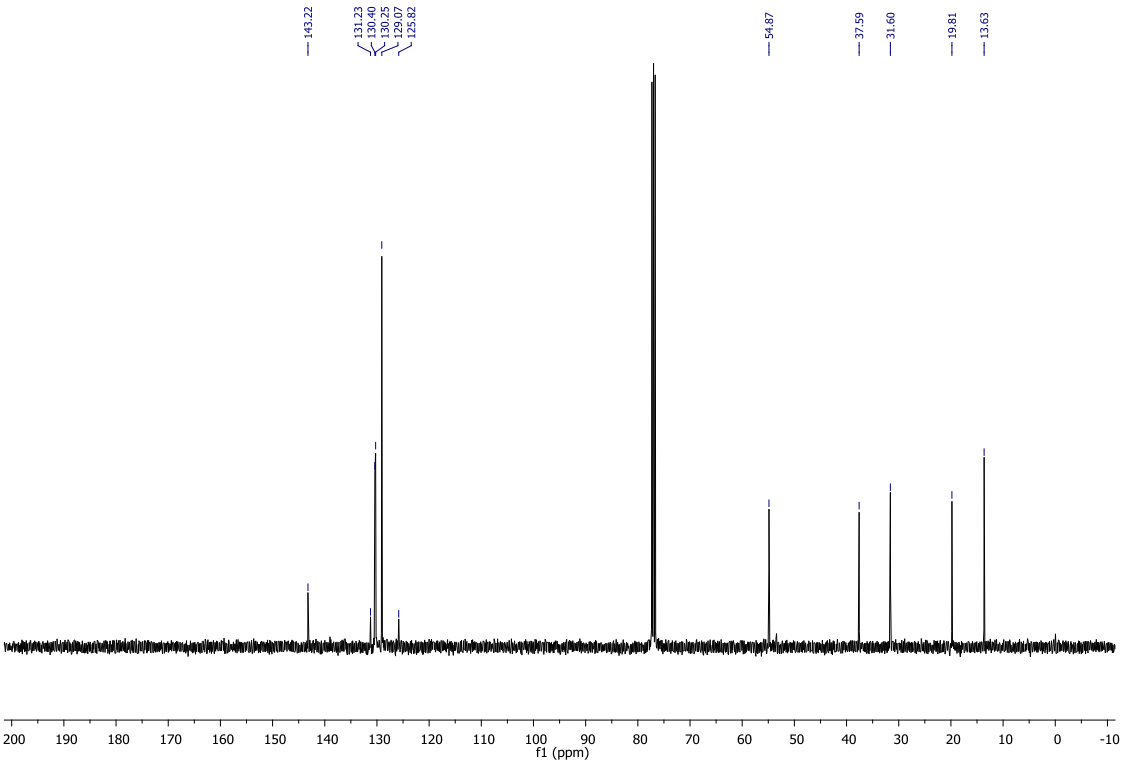

Figure S13. ^{13}C NMR spectra of **3c**

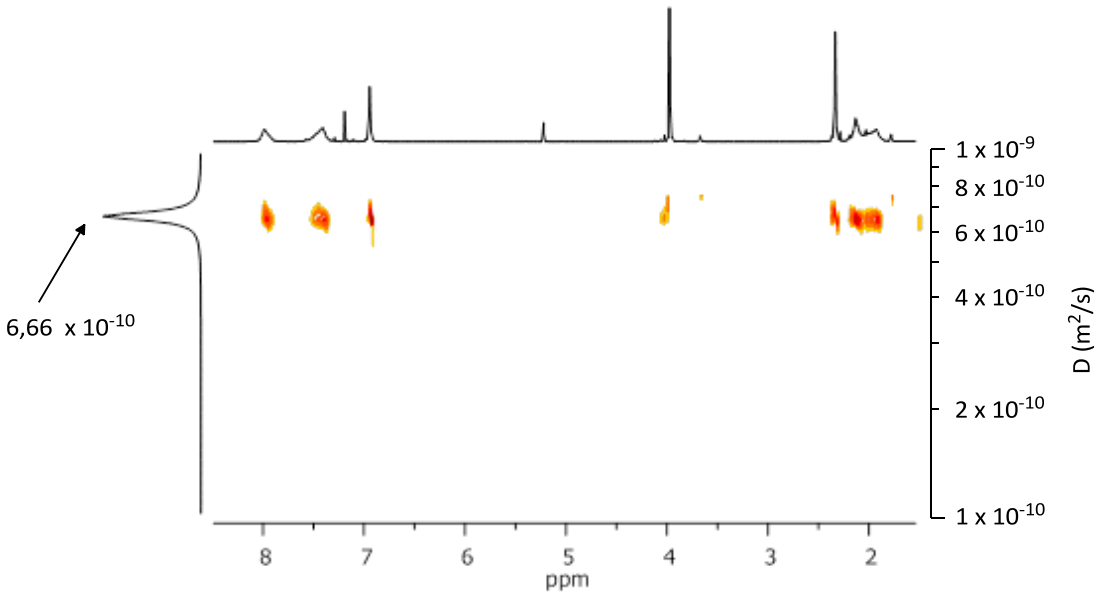

Figure S14. ^{1}H DOSY NMR spectrum of **3a** ($CDCl_3$)

5. Calculations of diffusion coefficients

Theoretical diffusion coefficients (*D)* have been calculated for DFT optimized structures of 3a - c, following the Einstein-Stokes equation, corrected by a factor derived from microfrictional theory[S11] and semi-empirically improved by Chen[S12] eq. (1), where *k* is Boltzmann's constant, *T* is the temperature, η is the viscosity of deutered chloroform (0.539 Cp [S13]). Spherical equivalent radii (R_{eq}) have been calculated from volumes limited by van der Waals surface (V^{vdW}) and volumes limited by Connolly surface (V^{SES}, SES – solvent excluded surface) following eq. (2), where M is the molecular weight of a solute and eq. (3) respectively. Van der Waals and Connolly volumes have been calculated by using Jmol software.[S14] Connolly surfaces have been generated with chloroform probe radius 2.3Å.[S15] Corrected by shape factor theoretical diffusion coefficients (D_f) were derived by means of using eq. (4) where *f(p)* is the shape factor and *p* is the geometrical factor for molecules regarded as ellipsoids ($p = a/b$, *a* – semi-major axis, *b* – semi-minor axis).[S16] Semi axes have been measured with GaussView 3.09 program. For all structures a prolate shape (with two short and one long axes) was assumed and calculated by eq. (5).

$$D = \left(\frac{kT}{6\pi\eta R_{eq}}\right)\left(1 + 0.695\left(\frac{Rs}{R_{eq}}\right)^{2.234}\right) \quad \text{(Eq. 1)}$$

$$R_{eq}^{vdW} = \sqrt[3]{\frac{3MV^{vdW}}{4\pi N_A}} \quad \text{(Eq. 2)}$$

$$R_{eq}^{SES} = \sqrt[3]{\frac{3MV^{SES}}{4\pi}}$$

(Eq. 3)

$$D_f = D \times f(p)$$

(Eq. 4)

$$f(p) = p^{\frac{1}{3}}(p^2 - 1)^{-\frac{1}{2}} ln\left[p + (p^2 - 1)^{\frac{1}{2}}\right]$$

(Eq. 5)

6. Computational details

All density functional theory (DFT) calculations were performed with Gaussian 03 program suite.[S17] The geometries of the complexes and ligands were optimized (tables, in the ESI†) by using B3LYP density functional theory and the 6-31G(d) basis sets on Cl, N, C, H atoms except Pd atoms (LanL2DZ basis set) implemented in the Gaussian 03.[S18,S19] The starting geometries of 3a - c complexes were generated from their crystal structures, whereas the starting geometries of adequate monomers were derived from their optimized complexes. Structures of all isomers of the calculated complexes were first optimized in vacuo.

Table S3. Energies of palladium species bearing tzNHC$^{Ph/Mes}$ ligand

	E (hartree)	ZPE (kcal/mol)
3a	-3817.61571497	424.18
3a *(cisoidal)*	-3817.60918482	424.25
monomeric	-1908.78446038	211.71

Table S4. Energies of possible equilibrium systems in relation to most stable dimer [{Pd(μ-Cl)Cl(tzNHC$^{Ph/Mes}$)}$_2$] (**3a***) (transoidal)*

	E (hartree)	ZPE (kcal/mol)	ΔE_{zpe} (kcal/mol)	ΔE_{zpe} (kJ/mol)
3a *(transoidal)*	-3817.61571497	424.18	0.00	0.00
3a *(cisoidal)*	-3817.60918482	424.25	4.16	17.41
2 × monomeric	-3817.56892076	423.42	28.60	119.67

Table S5. Energies of palladium species bearing tzNHC$^{Ph/Hex}$ ligand.

	E (hartree)	ZPE (kcal/mol)
3b *(transoidal)*	-3591.39702819	434.15
3b *(cisoidal)*	-3591.38776995	433.77
monomeric	-1795.67314283	216.42

Table S6. Energies of possible equilibrium systems in relation to most stable dimer [{Pd(μ-Cl)Cl(tzNHC$^{Ph/Hex}$)}$_2$] (**3b**) *(transoidal)*

	E (hartree)	ZPE (kcal/mol)	ΔE_{zpe} (kcal/mol)	ΔE_{zpe} (kJ/mol)
***3b** (transoidal)*	-3591.39702819	434.15	0.00	0.00
***3b** (cisoidal)*	-3591.38776995	433.77	5.43	22.73
2 × monomeric	-3591.34628566	432.84	30.53	127.74

Table S7. Energies of palladium species with bearing tzNHC$^{Ph/But}$ ligand.

	E (hartree)	ZPE (kcal/mol)
***3c** (transoidal)*	-3434.14441533	362.16
***3c** (cisoidal)*	-3434.13867638	361.94
monomeric	-1717.04694654	180.60

Table S8. Energies of possible equilibrium systems in relation to most stable dimer [{Pd(μ-Cl)Cl(tzNHC$^{Ph/But}$)}$_2$] (**3c**) *(transoidal)*

	E (hartree)	ZPE (kcal/mol)	ΔE_{zpe} (kcal/mol)	ΔE_{zpe} (kJ/mol)
***3c** (transoidal)*	-3434.14441533	362.16	0.00	0.00
***3c** (cisoidal)*	-3434.13867638	361.94	3.39	14.18
2 × monomeric	-3434.09389308	361.19	30.74	128.61

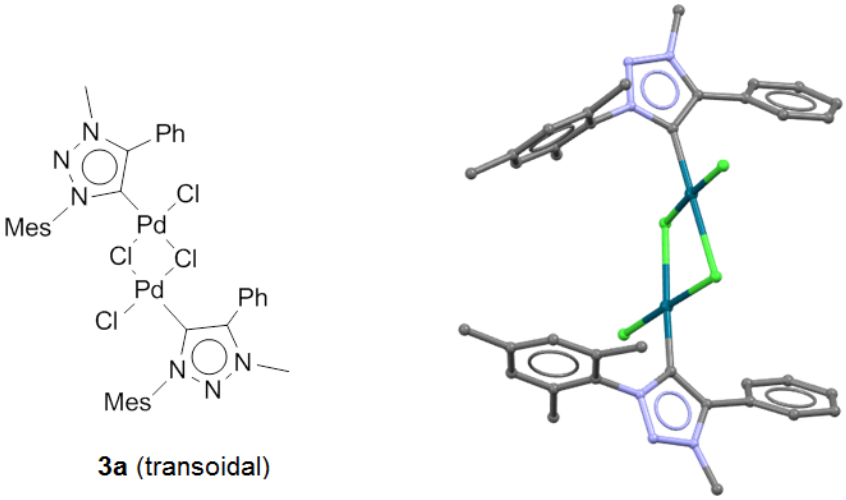

3a (transoidal)

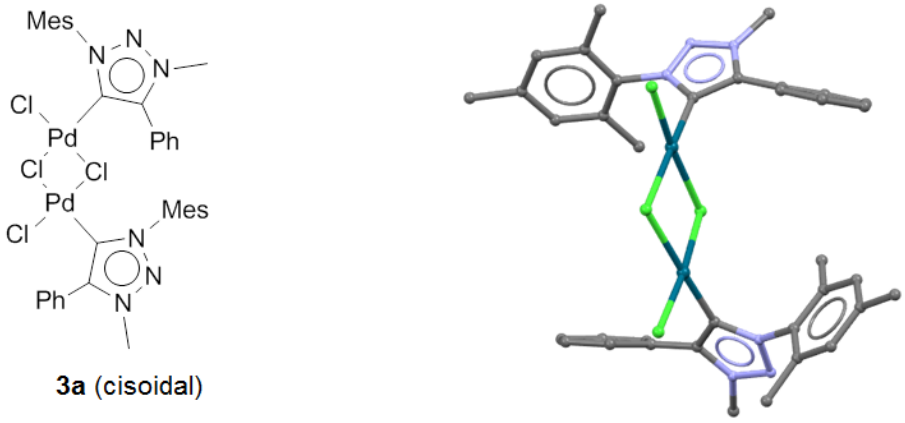

3a (cisoidal)

$(tzNHC^{Ph/Mes})PdCl_2$

Figure S15. Structures of Pd species bearing $tzNHC^{Ph/Mes}$ ligand (schematic on left, DFT optimised on right).

7. The study of transformation of 3a in solution

Table S9. Energies of palladium species bearing tzNHC$^{Ph/Mes}$ ligand.

	E (hartree)	ZPE (kcal/mol)
***3a** (transoidal)*	-3817.61571497	424.18
***3a** (cisoidal)*	-3817.60918482	424.25
2 × monomeric	-1908.78446038	211.71
4	-2770.37457158	422.01

Table S10. Van der Waals volumes V^{vdW}, Connolly volumes V^{SES}, theoretical diffusion coefficients D^{vdW}, D^{SES} and theoretical diffusion coefficients corrected by shape factor D_f^{vdW}, D_f^{SES} for DFT optimized structures of Pd species.

	V^{vdW} [Å^3]	V^{SES} [Å^3]	D^{vdW} [10^{-10} m^2/s]	D^{SES} [10^{-10} m^2/s]	D_f^{vdW} [10^{-10} m^2/s]	D_f^{SES} [10^{-10} m^2/s]	D_f^{exp} [10^{-10} m^2/s]
***3a** (transoidal)*	631.61	794.09	6.20	6.68	5.99	6.45	6.66
***3a** (cisoidal)*	631.95	790.36	6.20	6.69	6.02	6.50	
monomeric	319.16	368.26	11.43	9.33	11.13	9.08	
4	571.86	668.63	7.05	7.17	7.04	7.16	7.63

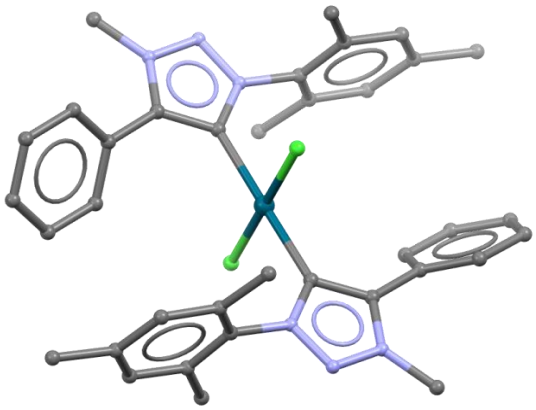

Figure S16. Optimized structure of **4**

8. Optimization of the conditions of Suzuki-Miyaura coupling

The 2 mL glass reactor equipped with a condenser and a magnetic stirring bar was charged in the air with p-tolylboronic acid (2.5×10^{-4} mol, 1.05 equiv) and 1 mL of ethanol (99.8 %). The reaction mixture was stirred at 22 °C for 5 min. until complete acid dissolution. Then, aryl halide (1 equiv), dodecane (internal standard), the appropriate amount of palladium complex and KOH (1.1 equiv) were added. The mixture was stirred at 22 °C or at reflux for 24 h. The reaction course was monitored by gas chromatography and GC/MS.

Table S11. Optimization of SM reaction catalysed by **3a**

Entry	Base	Solvent	**3a** (mol%)	Yield[a] [%]
1	TBAF	*i*-PrOH	1	66
2	KOH	*i*-PrOH	1	88
3	tBuOK	*i*-PrOH	1	33
4	K_2CO_3	*i*-PrOH	1	75
5	HCOONa	*i*-PrOH	1	traces
6	NaOH	*i*-PrOH	1	51
7	KOH	dioxane	1	traces
8	KOH	toluene	1	88
9	KOH	EtOH	1	98
10	KOH	EtOH	0.1	98
11	KOH	EtOH	0.1	97[b]
12	KOH	EtOH	0.05	76

Reaction conditions: 22 °C, 24 h, [ArBr]:[$ArB(OH)_2$]:[KOH] = 1:1.05:1.1; air; [a] yield calculated on the basis of GC analysis; [b] inert atmosphere.

9. Mass spectrometric study of the decomposition of 3a and 3b

The 2 mL glass reactor equipped with a condenser and a magnetic stirring bar was charged in the air with boronic acid (2.5×10^{-4} mol,1.0 equiv) and 1 mL of ethanol The reaction mixture was stirred at 22 °C for 5 min. until complete acid dissolution. Then, the appropriate amount of palladium complex **3a** or **3b** (0.1 mol%) and KOH (1.1 equiv) were added. Five minutes after addition of catalyst reaction mixture was diluted in appropriate amount of methanol and injected to ESI-MS. No signals above m/z=1000 was observed.

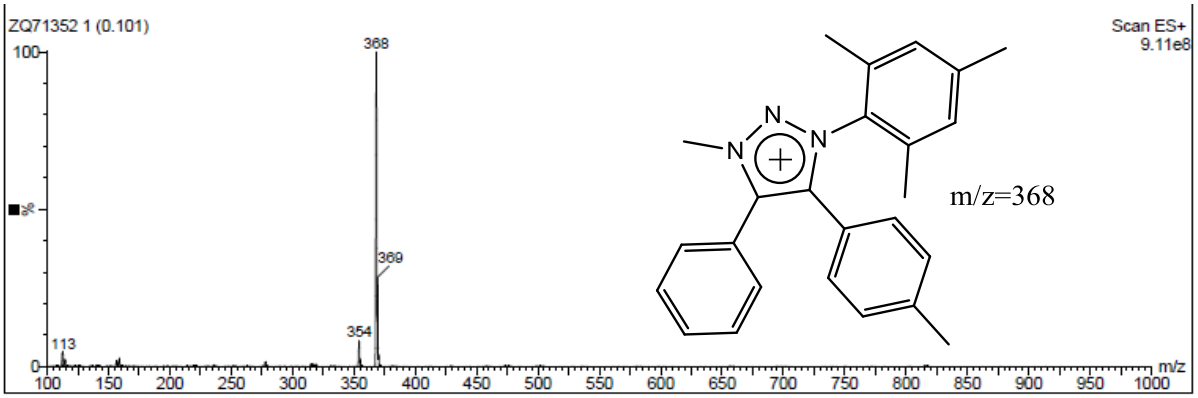

Figure S17. Treatment of **3a** with boronic acid **6**. Mass spectra of the reaction mixture.

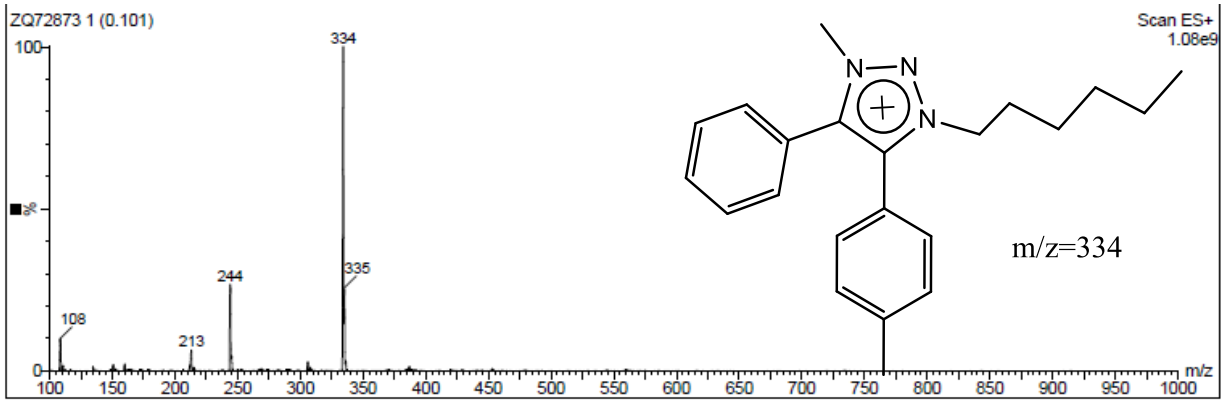

Figure S18. Treatment of **3b** with boronic acid **6**. Mass spectra of the reaction mixture.

10. ^{1}H NMR spectroscopic investigation of the reaction of 3a with tolylboronic acid

In the NMR tube **3a** (15 mg) and 1,3,5-trimethoxybenzene (internal standard) were dissolved in $CDCl_3$. Then *p*-tolylboronic acid (2 equiv) KOH (2 equiv) and 3 μL of distilled water were added. The reaction course was monitored by ^{1}H NMR spectroscopy.

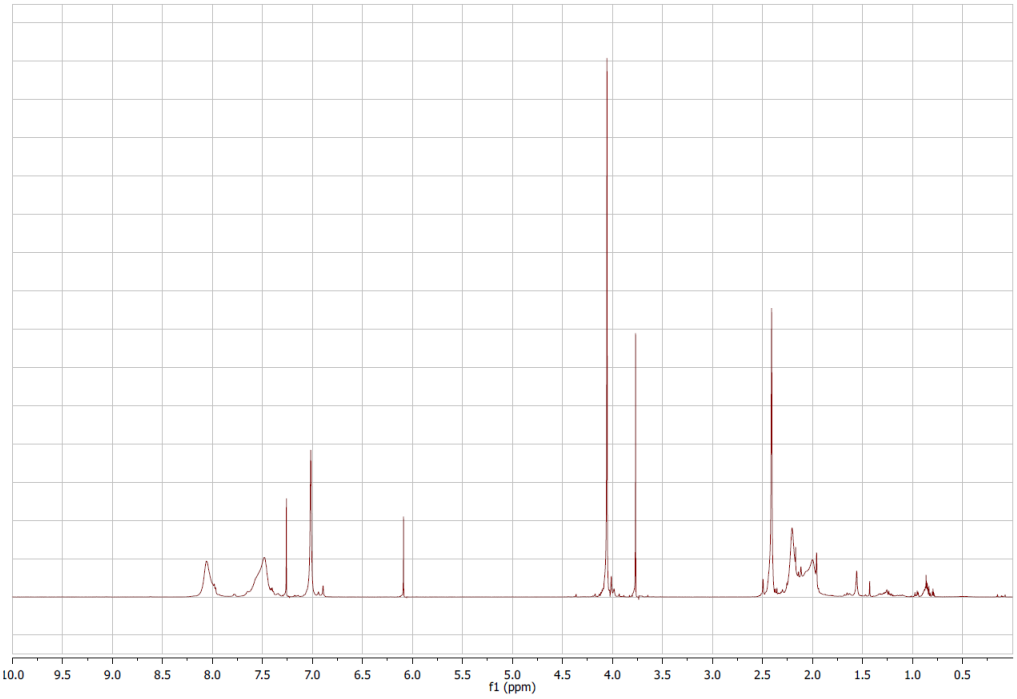

Figure S19. ^{1}H NMR spectrum of the reaction mixture before the addition of tolylboronic acid.

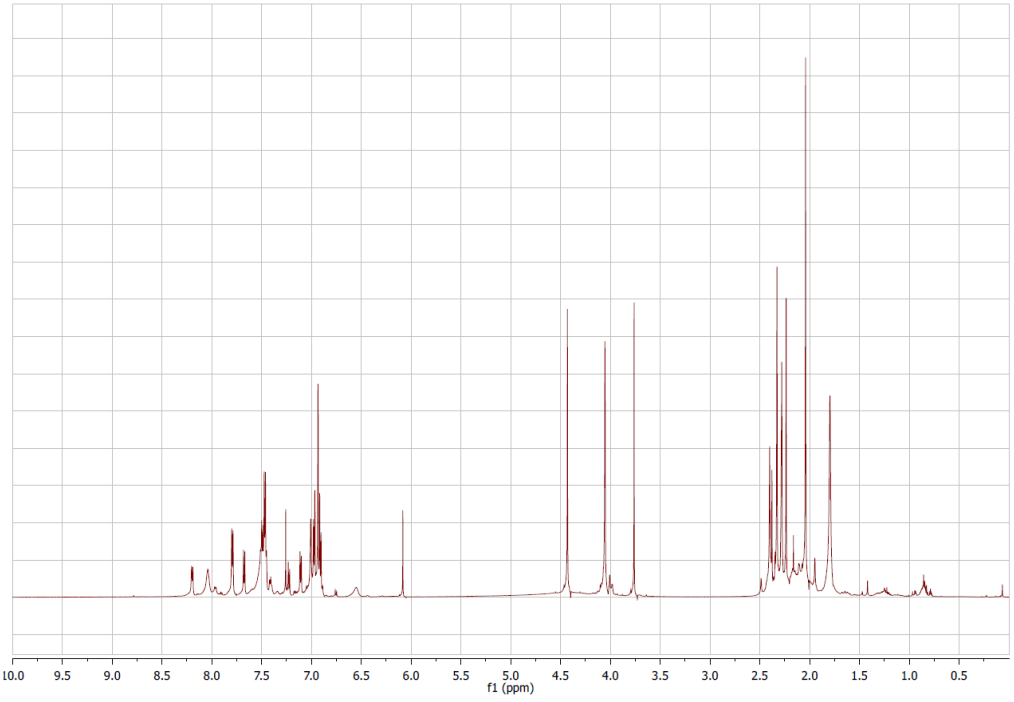

Figure S20. ^{1}H NMR spectrum of the reaction mixture 30 min after addition of tolylboronic acid.

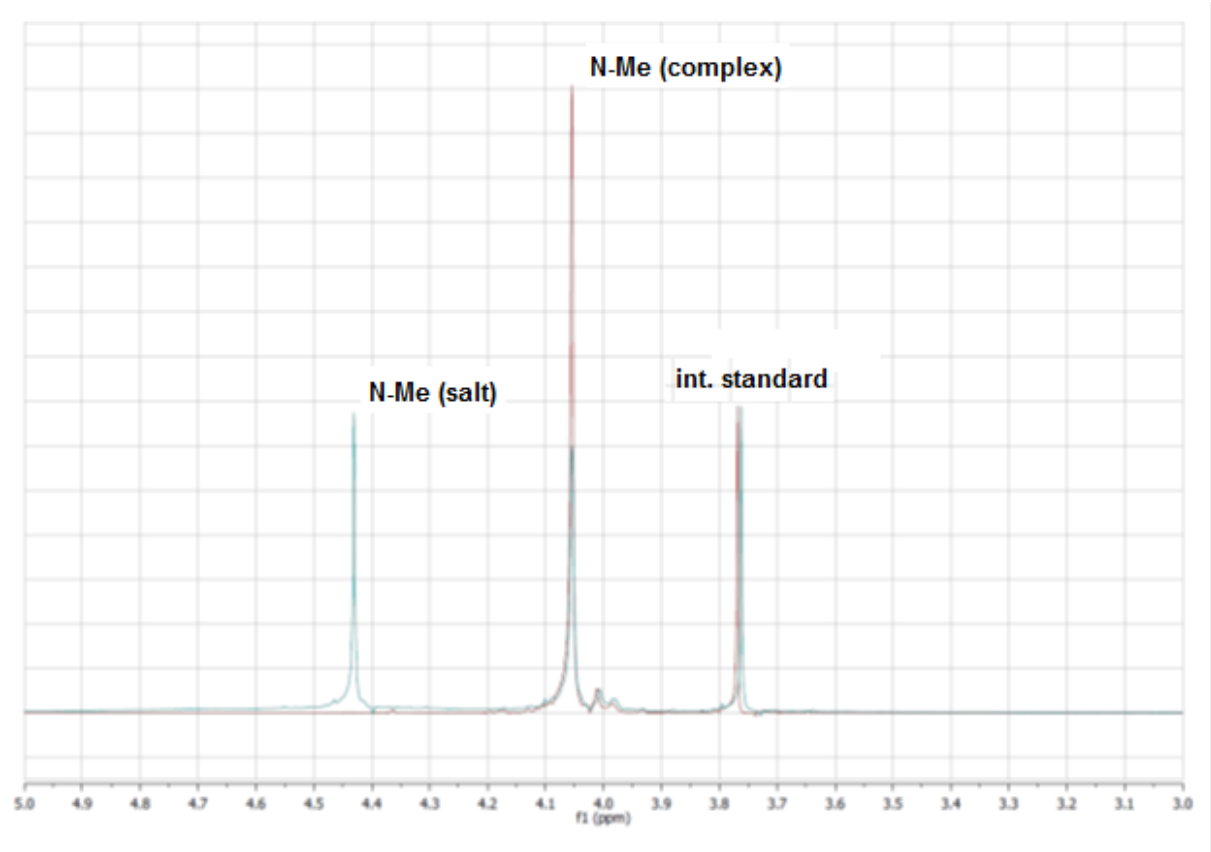

Figure S21. Superimposed spectra.

11. Synthesis and characterization of 8

Complex **3a** (100 mg) was dissolved in ethanol (5 mL) in a 25 mL round bottomed flask equipped with a magnetic stirring bar and a stopcock. Then, phenylboronicacid (4 equiv) was added followed by potassium hydroxide (4 equiv). Reaction mixture was then stirred overnight (18 h). Upon the reaction progress the mixture changed from bright yellow solution into black mixture with noticeable participation of palladium black. After the completion of reaction mixture was filtered through short pad of celite, and filter was washed with methanol sever times (3 × 10 mL). Combined organic solutions was evaporated to dryness and pure product 20.13 mg was isolated in 23 % yield by column chromatograhy (DCM-DCM/iso-PrOH gradually from 1 % to 10 % for every 50 mL of solvent, v/v, Rf = 0.3). Notably, use of methanol as a mobile phase was unsuccessful due to the similar Rf of the unreacted **3a** and the isolated salt **8**.

^{1}H NMR (403 MHz, $CDCl_3$) δ 7.35-7.31 (m, *2*), 7.19-7.16 (m, 3H), 6.98 (d, *J* = 7.5 Hz, 4H), 6.82 (s, 2H), 4.33 (s, 3H), 2.27 (s, 3H), 1.99 (s, 3H), 1.80 (s, 3H), 1.76 (s, 3H); ^{13}C NMR (75 MHz, $CDCl_3$) δ 166.7, 146.5, 140.8, 135.8, 134.4, 129.83 (overlapping), 129,80 (overlapping) 129.6, 129.5, 128.9, 128.7, 128.5, 127.1, 117.5, 39.0, 21.3, 18.0, 17.9; HRMS: m/z calcd. for $C_{25}H_{26}N_3^+$ $[M–Cl]^+$ 368.2122; found 368.2122; Anal. calcd. for $C_{25}H_{26}ClN_3$: C, 74.33; H, 6.49; Cl, 8.78; N, 10.40. Found: C, 73.47; H, 6.63; Cl, 8.55; N, 10.12.

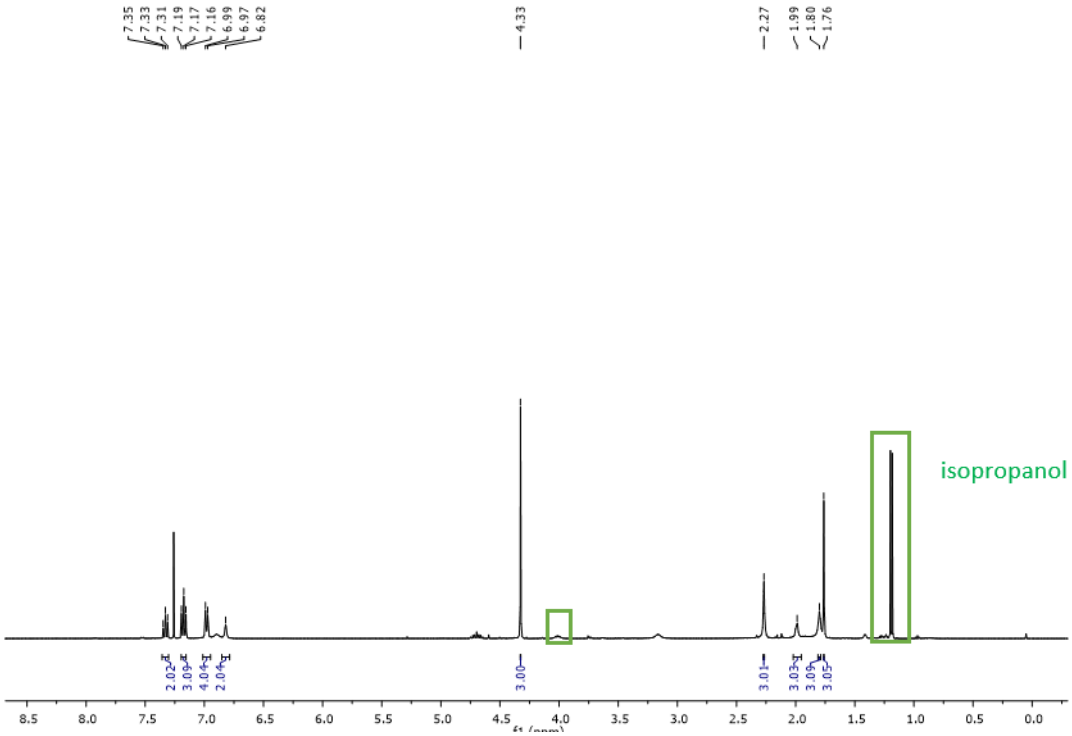

Figure S22 ^{1}H NMR of **8** ($CDCl_3$)

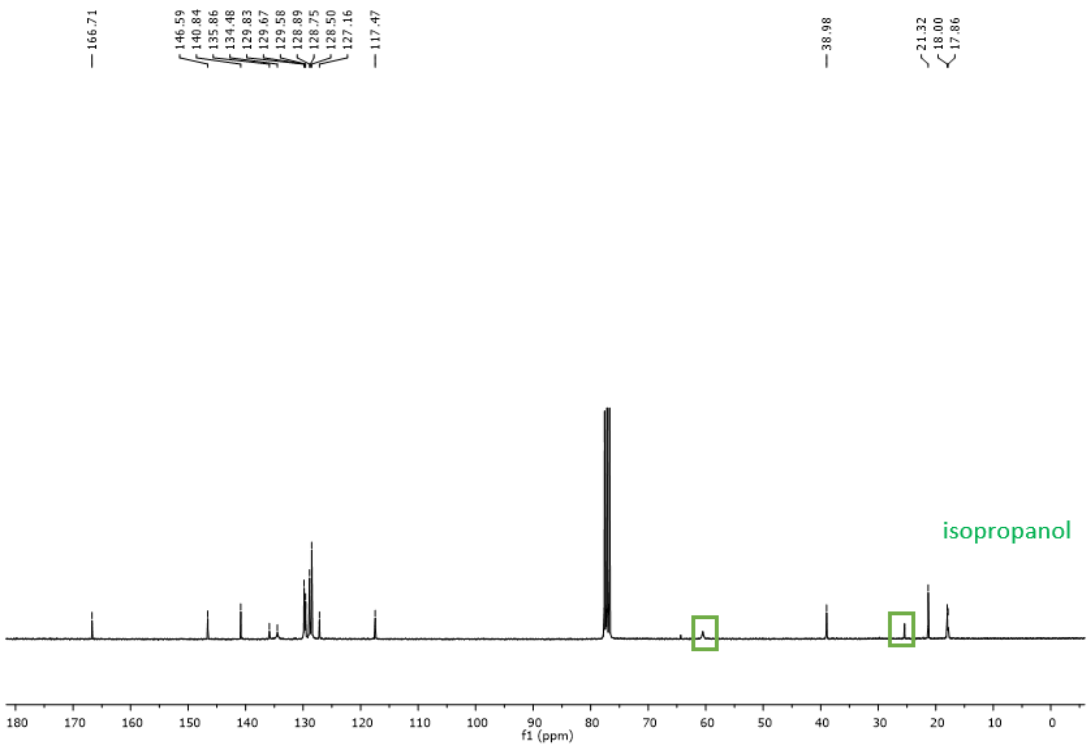

Figure S23 ^{13}C NMR of **8** ($CDCl_3$)

12. Mercury poisoning experiments

The glass flask (2 mL) with a condenser and a magnetic stirring bar was charged in the air with *p*-tolylboronic acid (2.5×10^{-4} mol, 1.05 equiv) and 1 mL of ethanol (99.8%). The reaction mixture was stirred at 22 °C for 5 min. until complete acid dissolution. Then, bromobenzene (2.38×10^{-4} mol, 1 equiv), dodecane (internal standard), palladium complex **3a** (2.5×10^{-7} mol, 0.1 mol%) and KOH (2.62×10^{-4} mol, 1.1 equiv) were added. Then, after 5 minutes, Hg (1000 equiv in relation to the catalyst) The reactions were carried upon vigorous stirring for 24 h. The reaction course was monitored by gas chromatography.

13. Transmission electron microscopy (TEM)

For Transmission electron microscopy (TEM) analysis a Jeol model JEM1200 EXII microscope was used. The 2 mL glass reactor equipped with a condenser and a magnetic stirring bar was charged in the air with boronic acid (2.5×10^{-4} mol, 1.05 equiv) and 1 mL of ethanol The reaction mixture was stirred at 22 °C for 5 min. until complete acid dissolution. Then, aryl halide (1 equiv), the appropriate amount of palladium complex 3a (0.1 mol%) and KOH (1.1 equiv) were added. The small drop from reaction mixture was placed on the copper grids with a pipette after 35 min and 2 hours respectively and measured. Representative TEM images were presented in Figures S24 and S25.

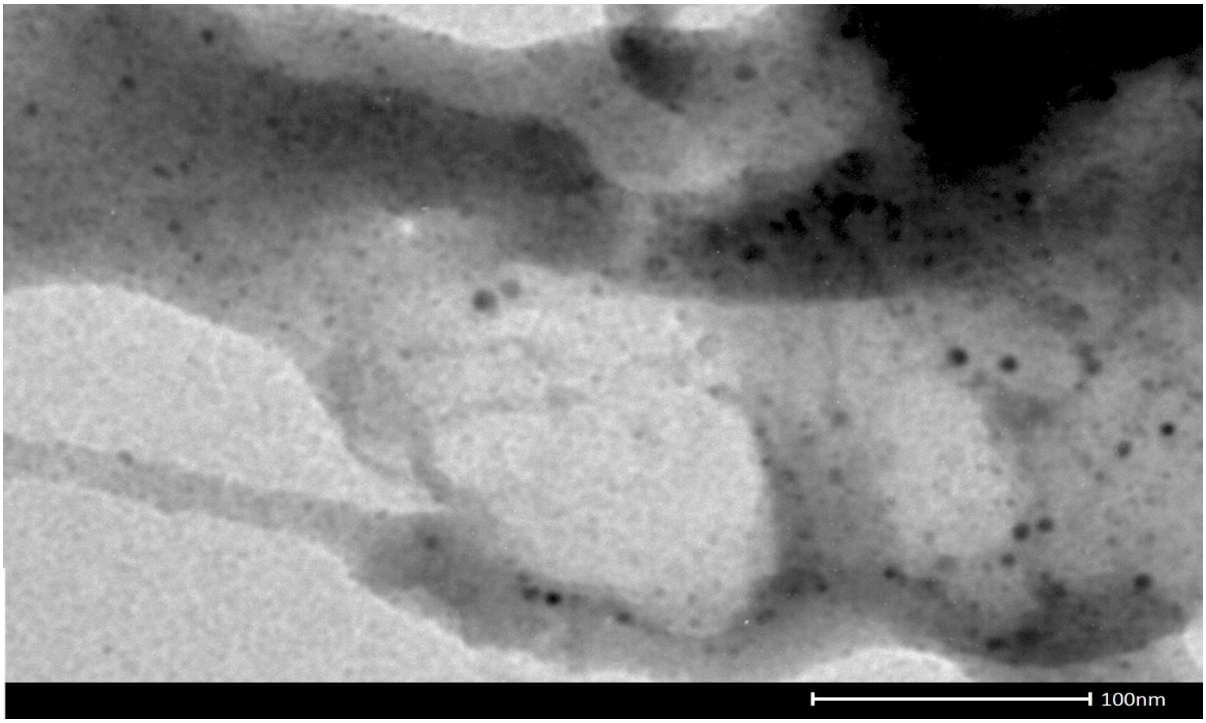

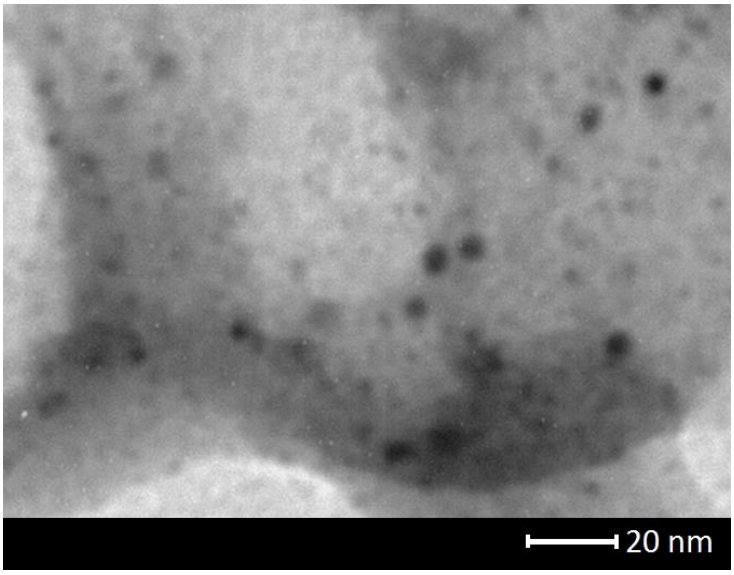

Figure S24. TEM micrographs of the particles present in reaction mixture after 35 min of the reaction course.

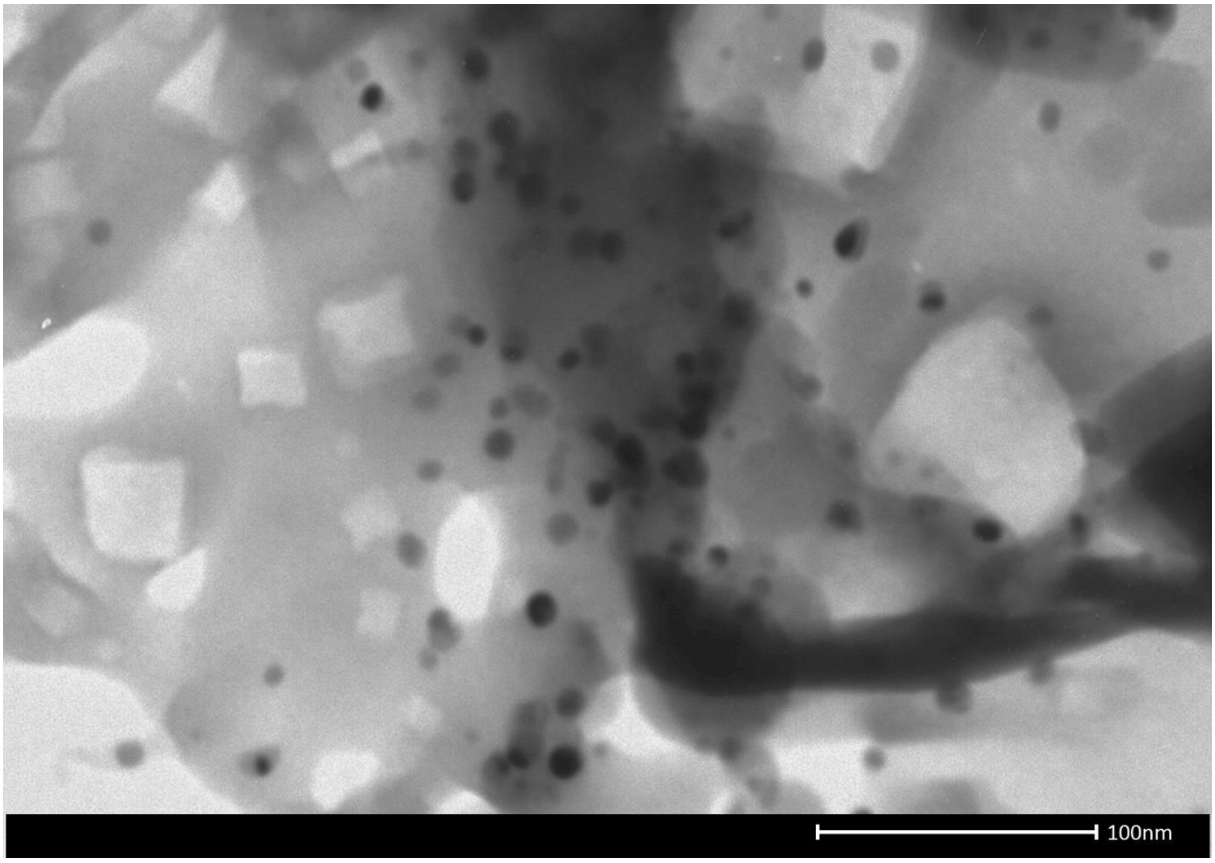

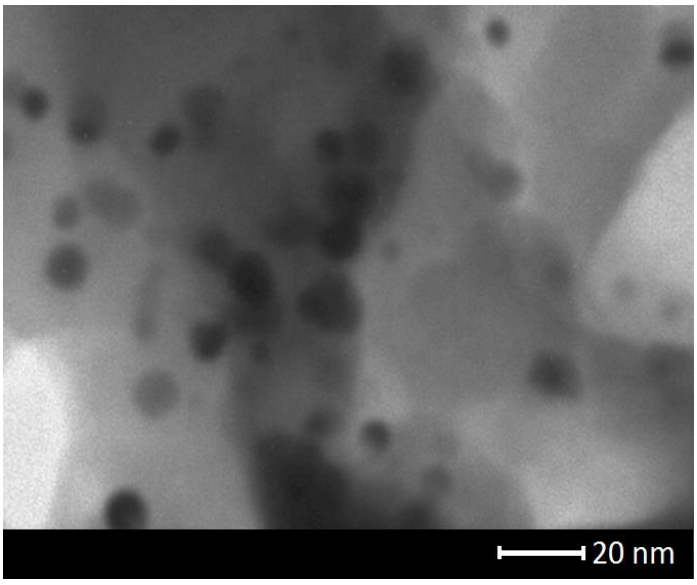

Figure S25. TEM micrographs of the particles present in reaction mixture after 2 h of the reaction course.

14. Synthesis and characterization of biaryls

The 2 mL glass reactor equipped with a condenser and a magnetic stirring bar was charged in the air with boronic acid (2.5×10^{-4} mol, 1.05 equiv) and 1 mL of ethanol (99.8 %). The reaction mixture was stirred at 22 °C for 5 min. until complete acid dissolution. Then, aryl halide (1 equivthe appropriate amount of palladium complex and KOH (1.1 equiv) were added. The mixture was stirred at 22 °C or at reflux for 24 h. Reaction products were identified on the basis of their mass spectra. All information on catalyst concentration refers to molar concentration of palladium. For isolation of products after reaction course 2 mL of distilled water and 2 mL of hexane were added. Organic layer was separated and treated as described below.

*4-Methylbiphenyl (**4a**)*

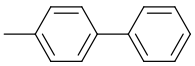

Yield 95%. White solid obtained after column chromatography (SiO_2, hexane); ^{1}H NMR (500 MHz, $CDCl_3$, ppm) δ: 7.79-7.75 (m, 2H), 7.68 (t, *J* = 7.6 Hz, 2H), 7.62 (dd, *J* = 10.5, 4.9 Hz, 2H), 7.52 (dd, *J* = 10.5, 4.2 Hz, 1H), 7.44 (d, *J* = 8.0 Hz, 2H), 2.59 (s, 3H). ^{13}C NMR: (101 MHz $CDCl_3$, ppm) 141.1, 138.3, 137.0, 129.4, 128.7, 127.0, 126.9 (2C), 21.1. MS (EI) m/z (%) = 168 (M^+, 100), 154 (47), 76 (21).

*4-chloro-4'-methylbiphenyl (**4b**)*

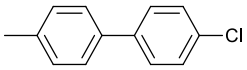

Yield 97%. White solid obtained after column chromatography (SiO_2, hexane/ethyl acetate 9/1) ^{1}H NMR (300 MHz, $CDCl_3$, ppm) δ: 7.54–7.40 (m, 6H), 7.28 (dd, *J* = 7.9, 0.6 Hz, 2H), 2.39 (s, 3H); ^{13}C NMR: (75 MHz, $CDCl_3$, ppm) δ:139.73, 137.56, 137.23, 133.16, 129.73, 128.98, 128.31, 126.94, 21.24. MS (EI) m/z (%) 202(M^+, 100) 201(15,4), 203(18,9), 204(28,9), 167(49,4), 166 (12,2), 165(25), 152(12).

*4-Methoxy-4'-methylbiphenyl (**4c**)*

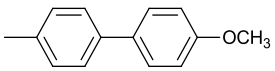

Yield 69%. White solid obtained after column chromatography (SiO_2, hexane/ethyl acetate 9/1) ^{1}H NMR (300 MHz, $CDCl_3$, ppm) δ: 7.54–7.50 (m, 2H), 7.46 (d, *J* = 8.1 Hz, 2H), 7.24 (d, *J* = 8.1 Hz, 2H), 7.00 –

6.96 (m, 2H), 3.85 (s, 3H), 2.39 (s, 3H); ^{13}C NMR: (75 MHz, $CDCl_3$, ppm) δ: 158.9, 137.9, 136.3, 133.7, 129.4, 127.9, 126.6, 114.1, 55.3, 21.0. MS (EI) m/z (%) = 198 (M^+, 100), 183 (47), 167 (50), 153 (24).

*2,4'-dimethylbiphenyl (**4d**)*

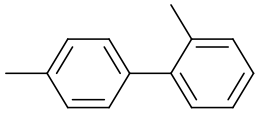

Yield 64%. Colourless oil obtained after column chromatography (SiO_2, hexane); ^{1}H NMR (400 MHz $CDCl_3$, ppm) δ: 7.35 (m, 8H), 2.41 (s, 3H), 2.28 (s, 3H). ^{13}C NMR: (100 MHz, $CDCl_3$, ppm) δ: 141.9, 138.4, 136.2, 135.0, 130.1, 129.8, 129.0, 128.5, 126.9, 125.4, 21.1, 20.5, MS (EI) m/z (%) = MS (EI) m/z (%) = 182 (M^+, 100), 167 (44), 153 (23), 91 (52).

*4-acetoxy-4'-methylbiphenyl (**4e**)*

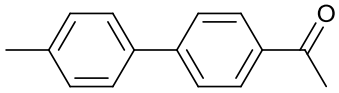

Yield 98%. White solid obtained after column chromatography (SiO_2, hexane/ethyl acetate 9/1); ^{1}H NMR (400 MHz, $CDCl_3$, ppm) δ: 8.02 (dd, *J* = 8.2, 0.5 Hz, 2H), 7.67 (dd, *J* = 8.2, 0.4 Hz, 2H), 7.55 – 7.52 (m, 2H), 7.28 (dd, *J* = 8.5, 0.6 Hz, 2H), 2.64 (s, 3H), 2.41 (s, 3H) ppm. ^{13}C NMR: (100 MHz, $CDCl_3$, ppm) δ: 197.7, 145.7, 138.2, 136.9, 135.6, 129.7, 128.9, 127.1, 126.9, 26.6, 21.2. MS (EI) m/z (%) = 210 (M^+, 100), 195 (73), 167 (53), 153 (37), 43 (23).

*2-(p-tolyl)pyridine (**4g**)*

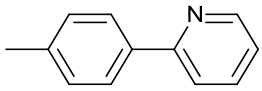

Yield 80%. colourless liquid, isolated by column chromatography (SiO_2, hexane/ethyl acetate 9/1), and subsequent extraction of combine fraction containing products with HCl aq. solution (1M, 5 mL)). Then, sodium biscarbonate was added to the aqueous layer till precipitate of white solid was formed. The reaction mixture was then extracted with hexane (3x5mL). Combine organic layers were dried over anhydrous $MgSO_4$ and product was obtained after evaporation of the solvent. ^{1}H NMR (400 MHz, $CDCl_3$, ppm) δ: 8.68 (ddd, *J* = 4.8, 1.7, 1.1 Hz, 1H), 7.91 – 7.87 (m, 2H), 7.76 – 7.68 (m, 2H), 7.32 – 7.27 (m,

2H), 7.22 - 7.18 (m, 1H), 2.41 (s, 3H). ^{13}C NMR: (100 MHz, $CDCl_3$, ppm) δ: 157.6, 149.7, 139.0, 136.8, 136.7, 129.6, 126.9, 121.9, 120.4, 21.4. δ: MS (EI) m/z (%) = 170 (M+H, 100), 171(13,5), 169 (32), 168 (31), 167 (14).

*3-(p-tolyl)pyridine (**4h**)*

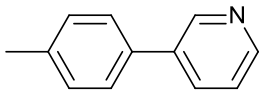

Yield 93%. White solid isolated by column chromatography (SiO_2, hexane/ethyl acetate 9/1), and subsequent extraction of combine fraction containing products with HCl aq. solution (1M, 5 mL)). Then, to the water layer sodium biscarbonate was added till participate of white solid. Mixture was then extracted with hexane (3 × 5 mL). Combine organic layers were dried over anhydrous $MgSO_4$ and product were obtained after evaporation of the solvent. ^{1}H NMR (400 MHz, $CDCl_3$, ppm) δ: 8.84 (d, *J* = 1.7 Hz, 1H), 8.57 (dd, *J* = 4.8, 1.6 Hz, 1H), 7.86 (ddd, *J* = 7.9, 2.4, 1.7 Hz, 1H), 7.48 (d, *J* = 8.1 Hz, 2H), 7.35 (ddd, *J* = 7.9, 4.8, 0.9 Hz, 1H), 7.29 (d, *J* = 7.8 Hz, 2H), 2.41 (s, 3H). ^{13}C NMR: (100 MHz, $CDCl_3$, ppm) δ: 148.27, 148.25, 138.19, 136.72, 135.03, 134.32, 129.94, 127.11, 123.66, 21.29. MS (EI) m/z (%) = 170 (M+H, 100), 169 (78), 168 (57), 167 (31), 115 (17).

15. NMR spectra of triazoles 1a-c and corresponding salts 2a-c

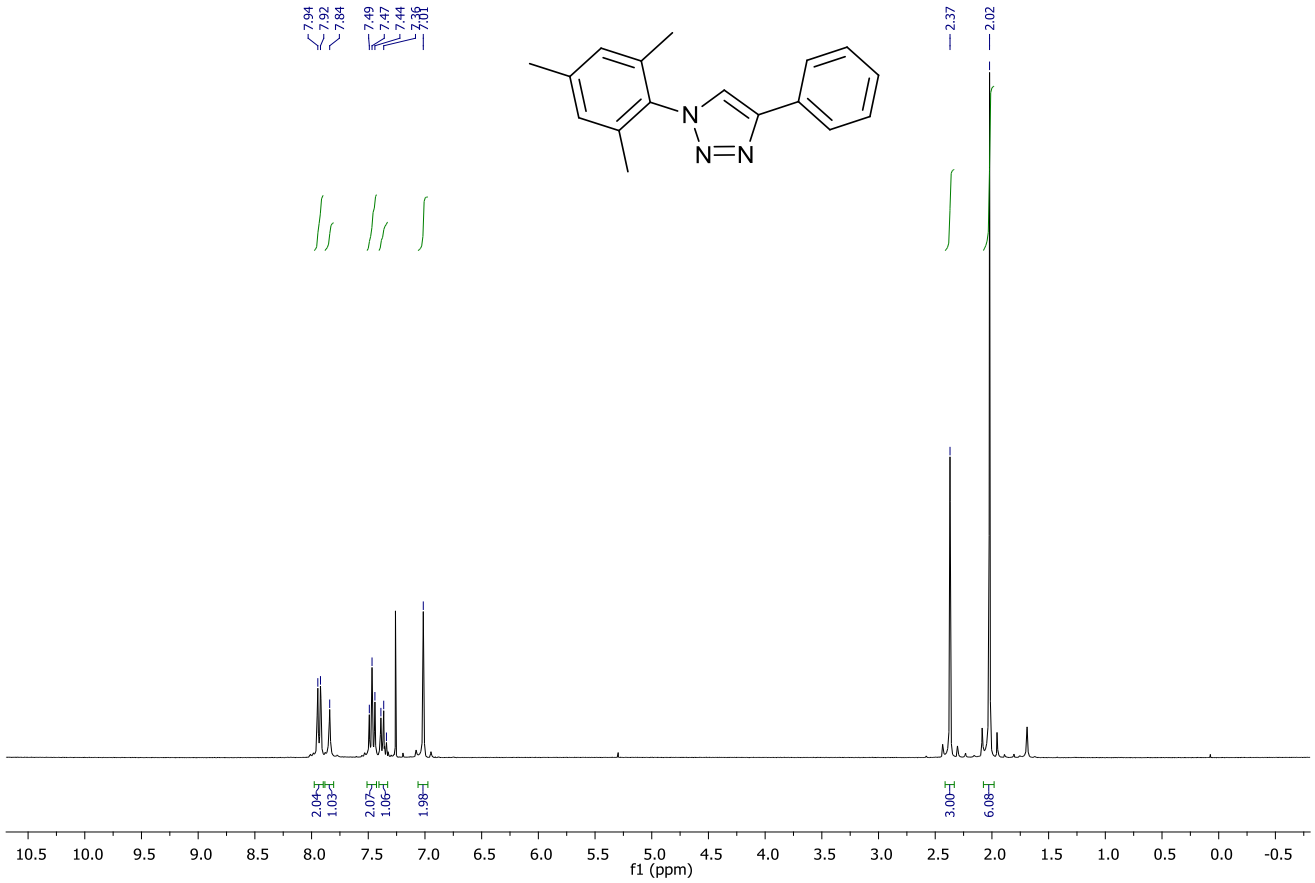

Figure S26. ^{1}H NMR spectra of 1-(2,4,6-trimethylphenyl)-4-phenyl-1*H*-1,2,3-triazole (**1a**)

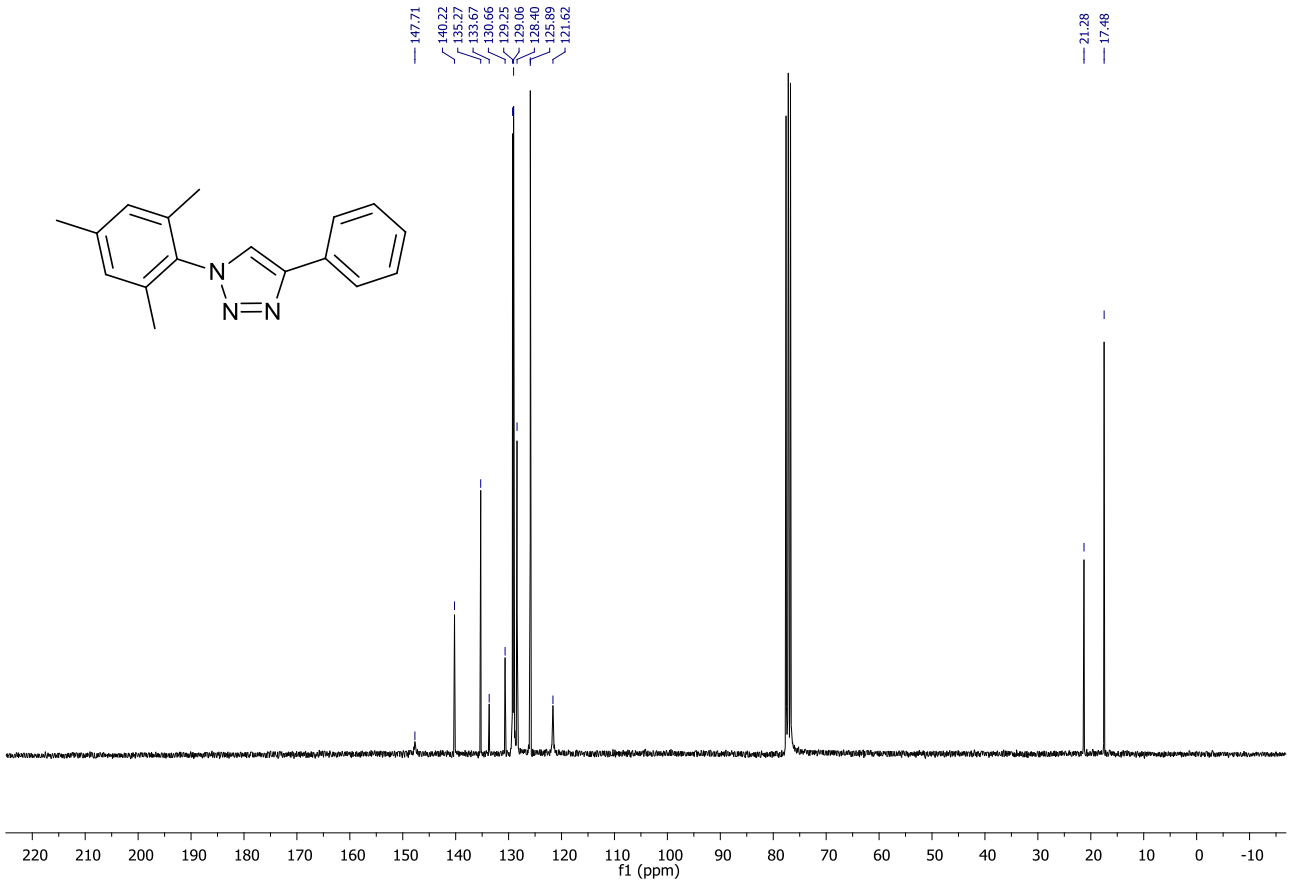

Figure S27. ^{13}C NMR spectra of 1-(2,4,6-trimethylphenyl)-4-phenyl-1*H*-1,2,3-triazole (**1a**)

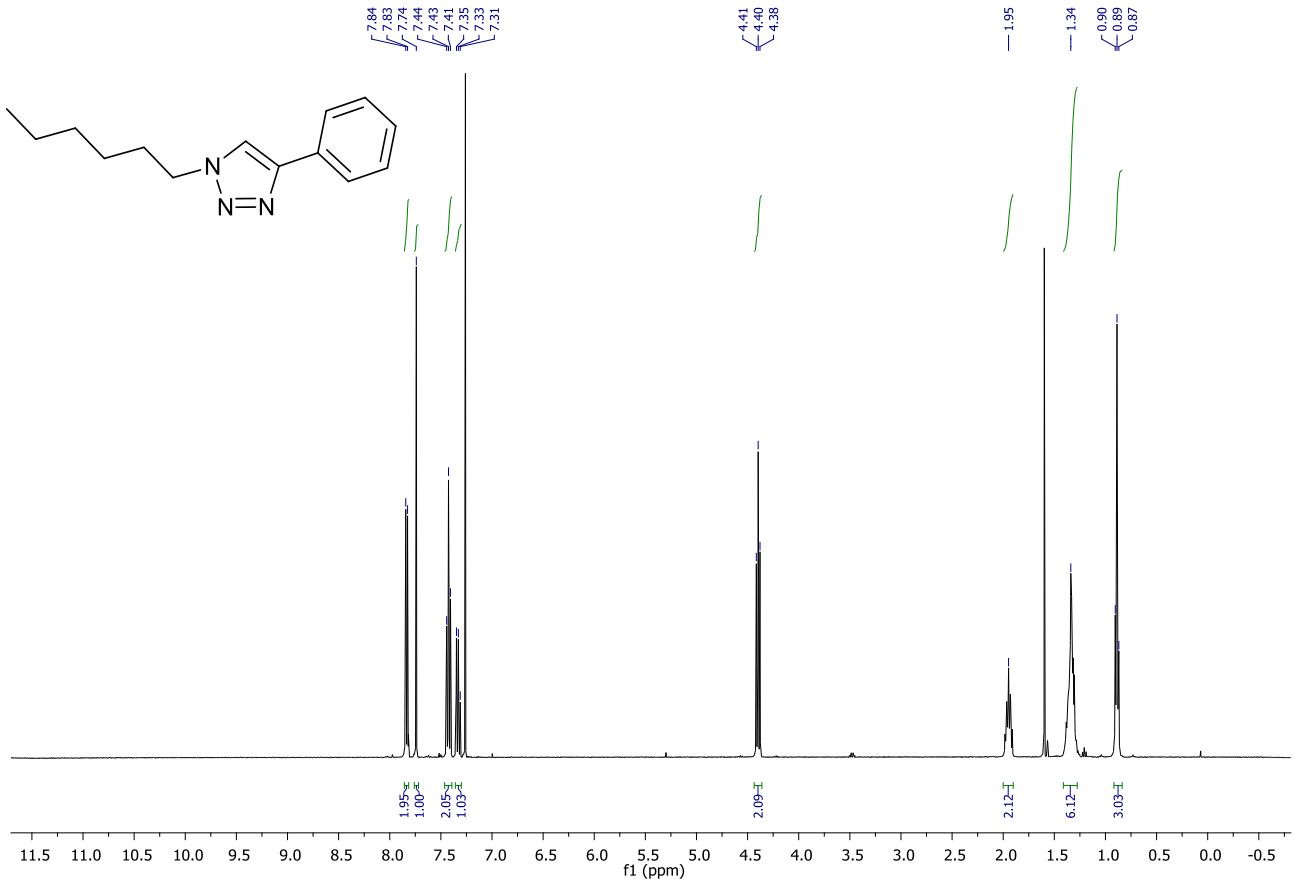

Figure S28. ^{1}H NMR spectra of 1-hexyl-4-phenyl-1*H*-1,2,3-triazole (**1b**)

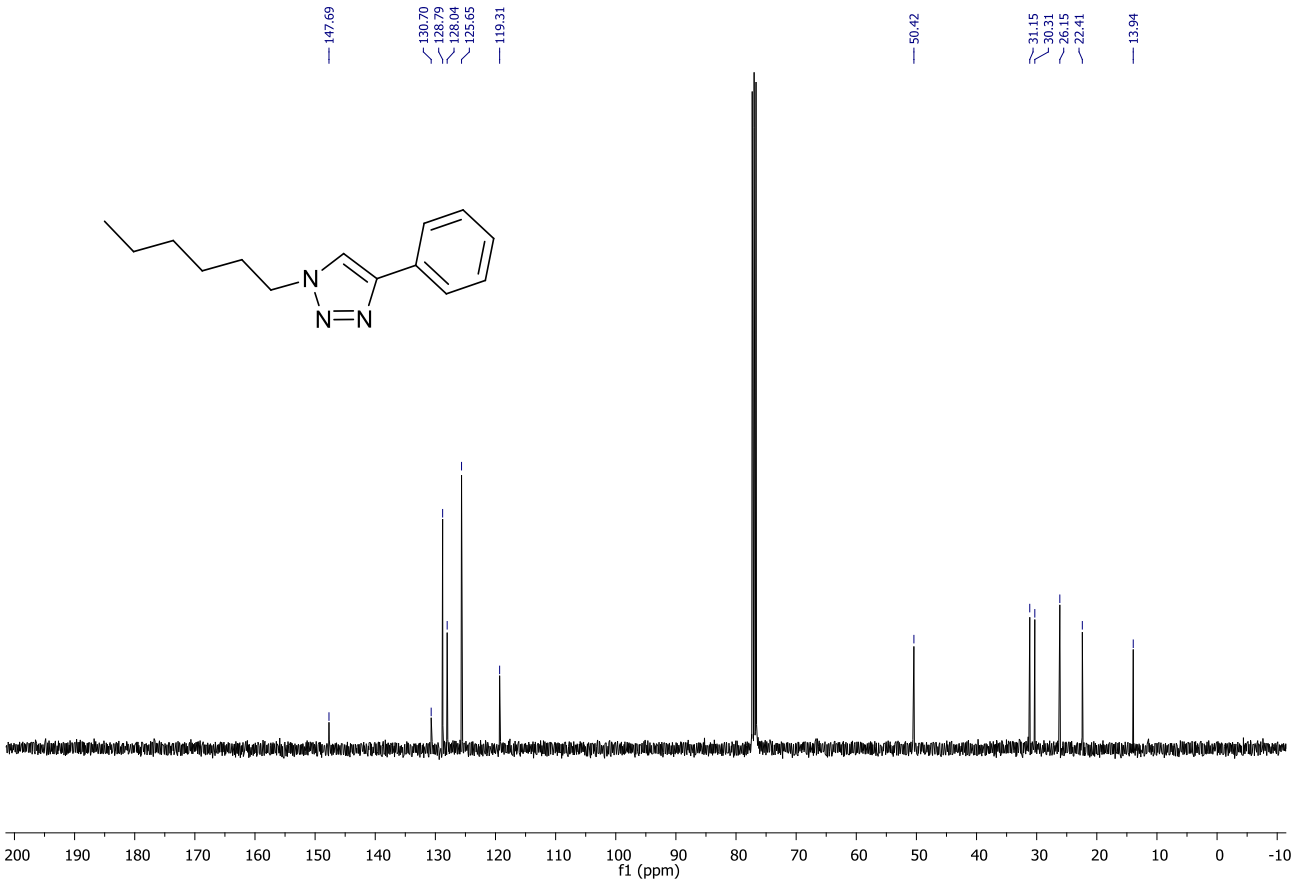

Figure S29. ^{13}C NMR spectra of 1-hexyl-4-phenyl-1*H*-1,2,3-triazole (**1b**)

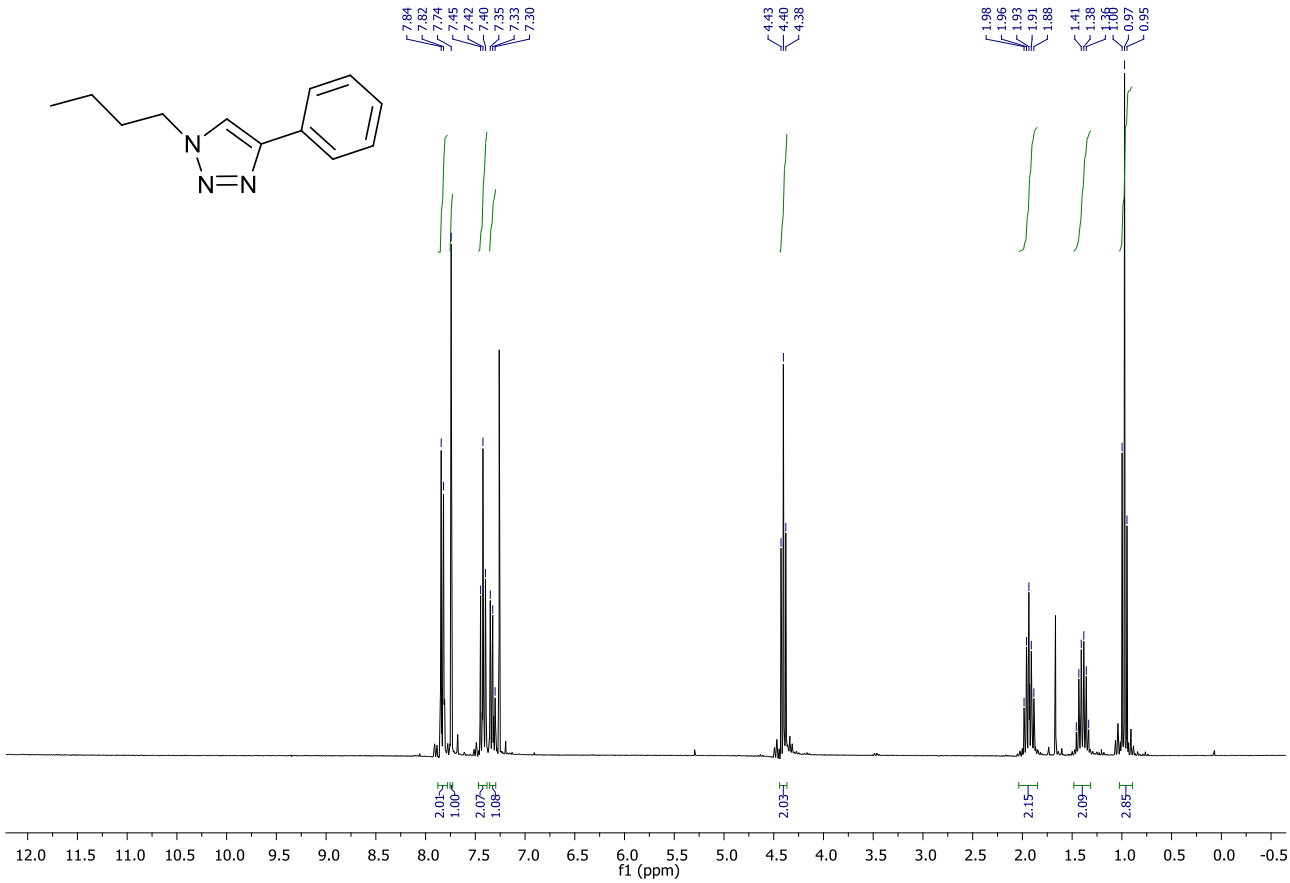

Figure S30. ^{1}H NMR spectra of 1-butyl-4-phenyl-1*H*-1,2,3-triazole (**1c**)

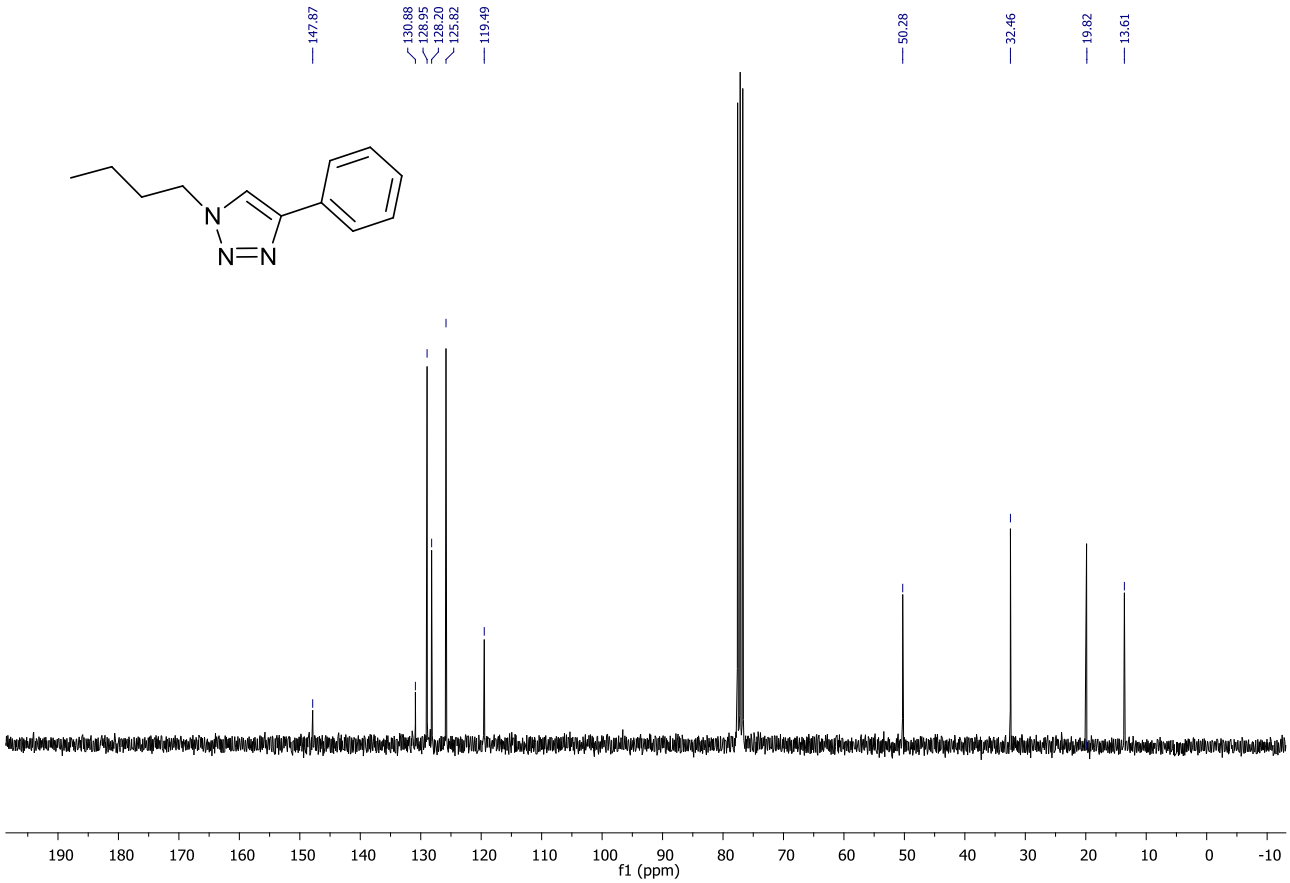

Figure S31. ^{13}C NMR spectra of 1-butyl-4-phenyl-1*H*-1,2,3-triazole (**1c**)

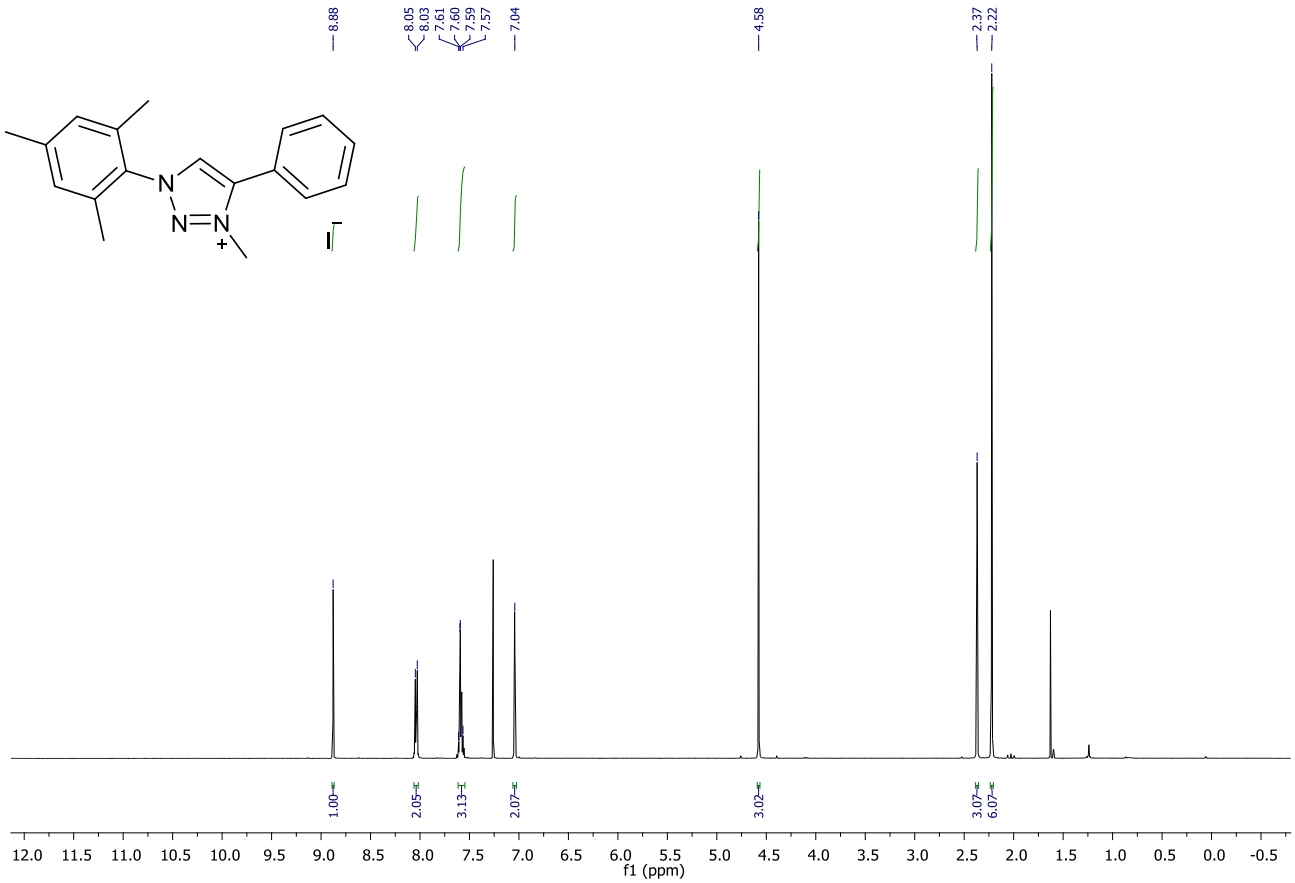

Figure S32. ^{1}H NMR spectra of 1-mesityl-3-methyl-4-phenyl-1*H*-1,2,3-triazolium iodide (**2a**)

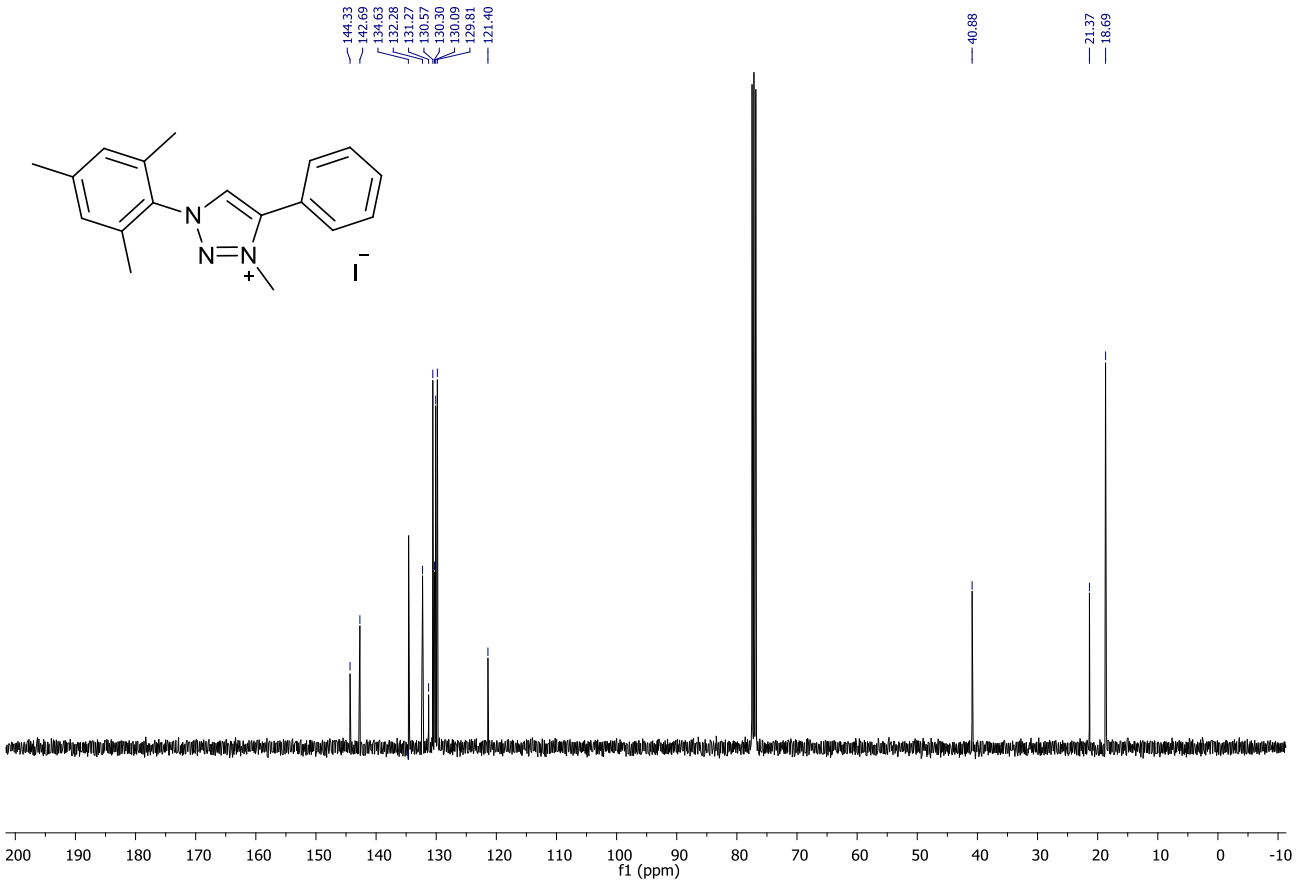

Figure S33. ^{13}C NMR spectra of 1-mesityl-3-methyl-4-phenyl-1*H*-1,2,3-triazolium iodide (**2a**)

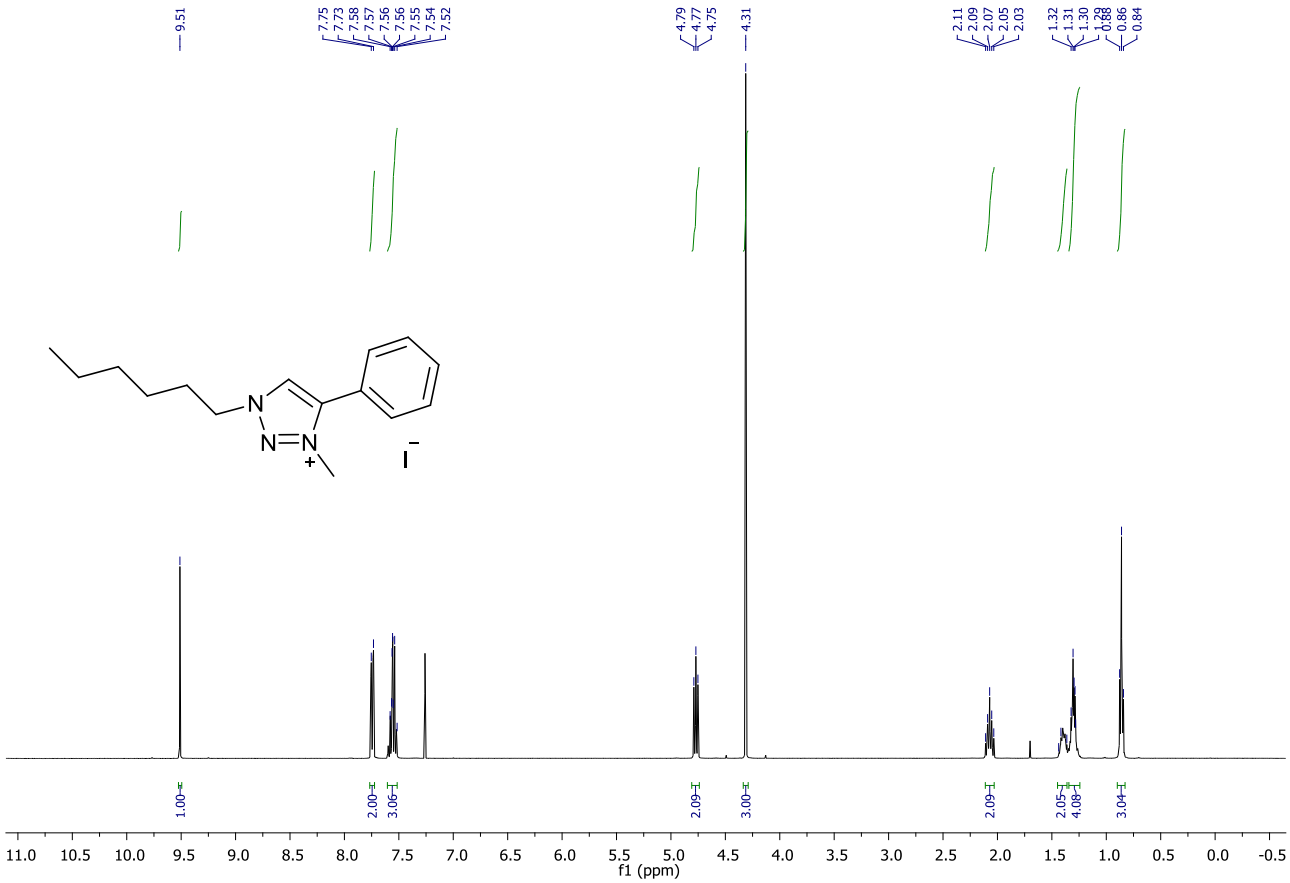

Figure S34. ^{1}H NMR spectra of 1-hexyl-3-methyl-4-phenyl-1*H*-1,2,3-triazolium iodide (**2b**)

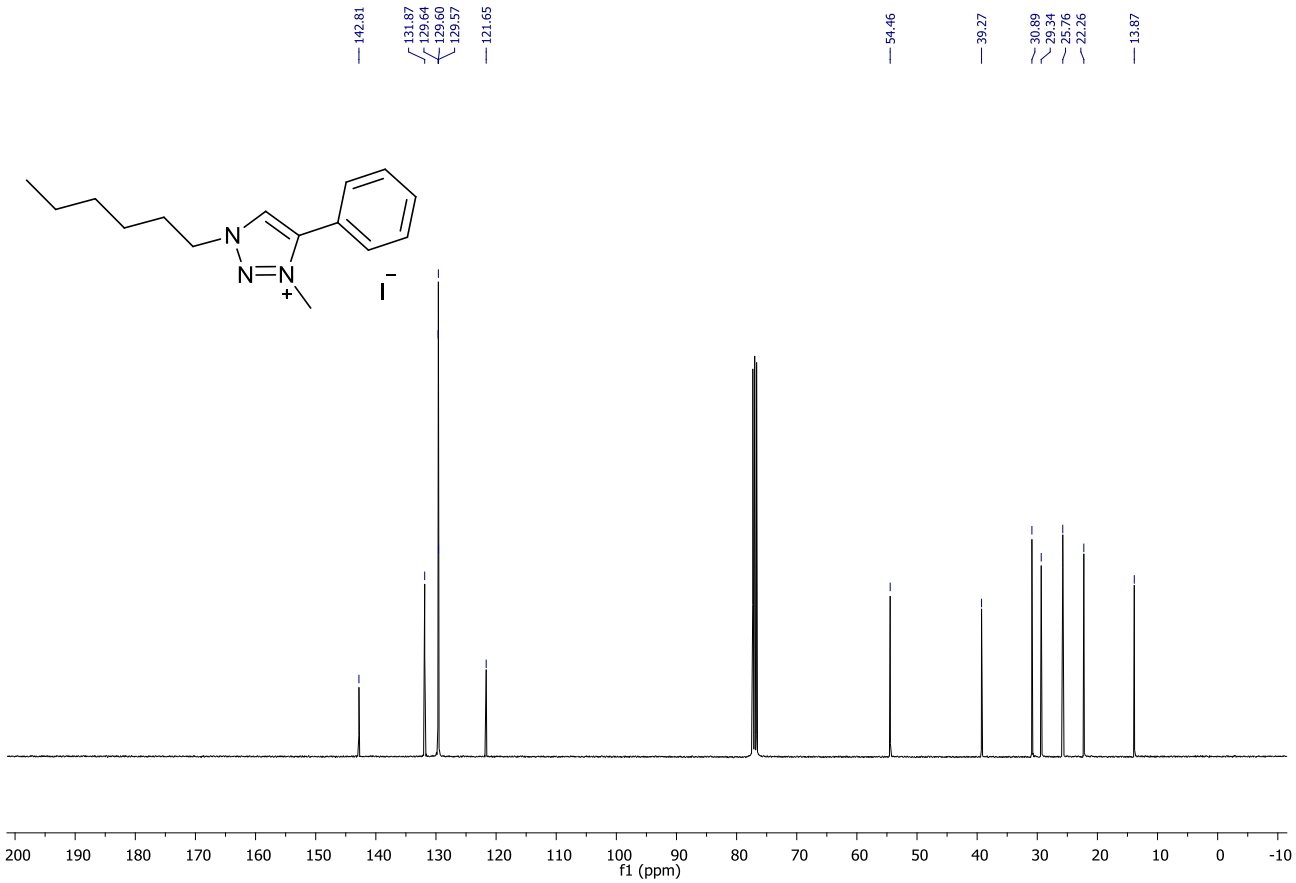

Figure S35. ^{13}C NMR spectra of 1-hexyl-3-methyl-4-phenyl-1*H*-1,2,3-triazolium iodide (**2b**)

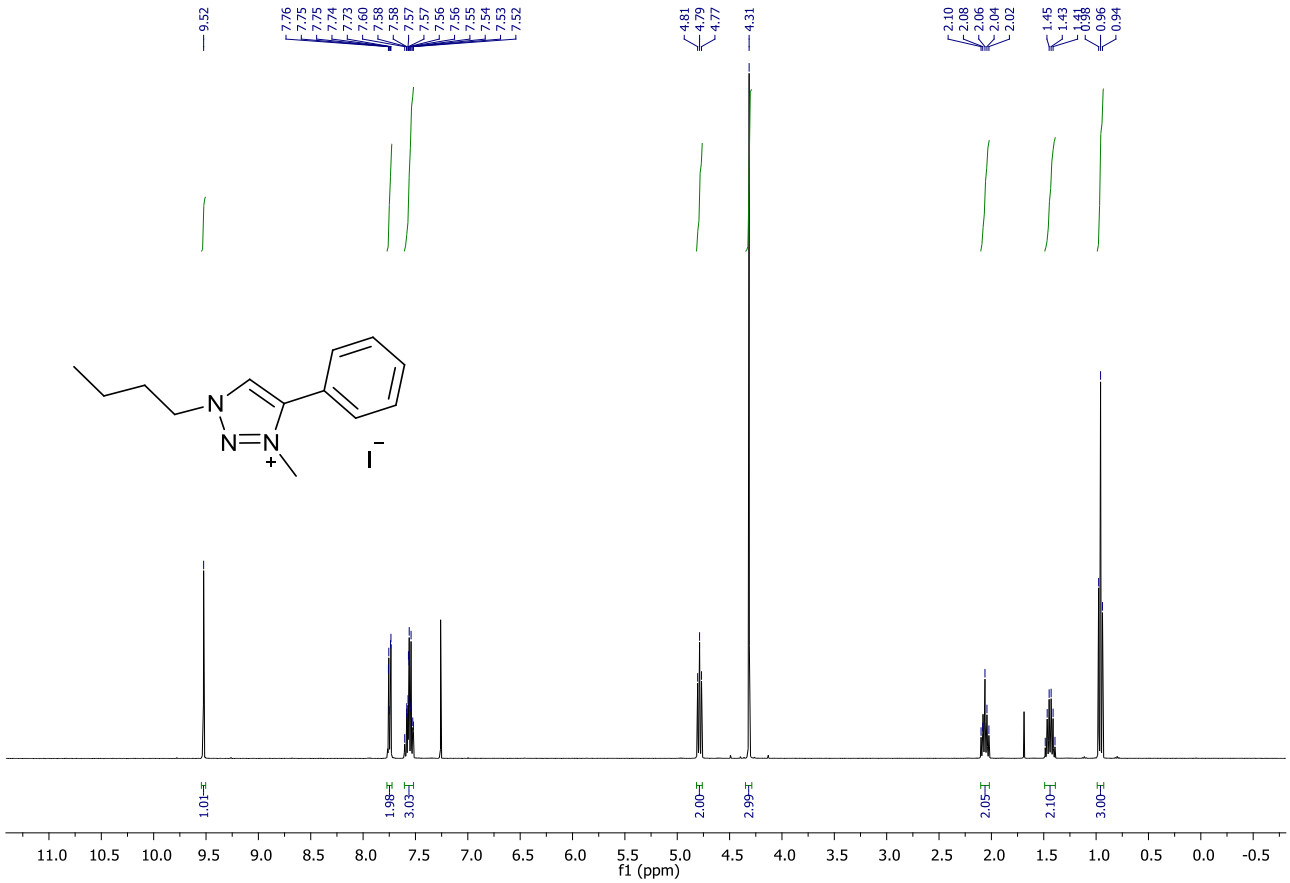

Figure S36. ^{1}H NMR spectra of 1-butyl-3-methyl-4-phenyl-1*H*-1,2,3-triazolium iodide (**2c**)

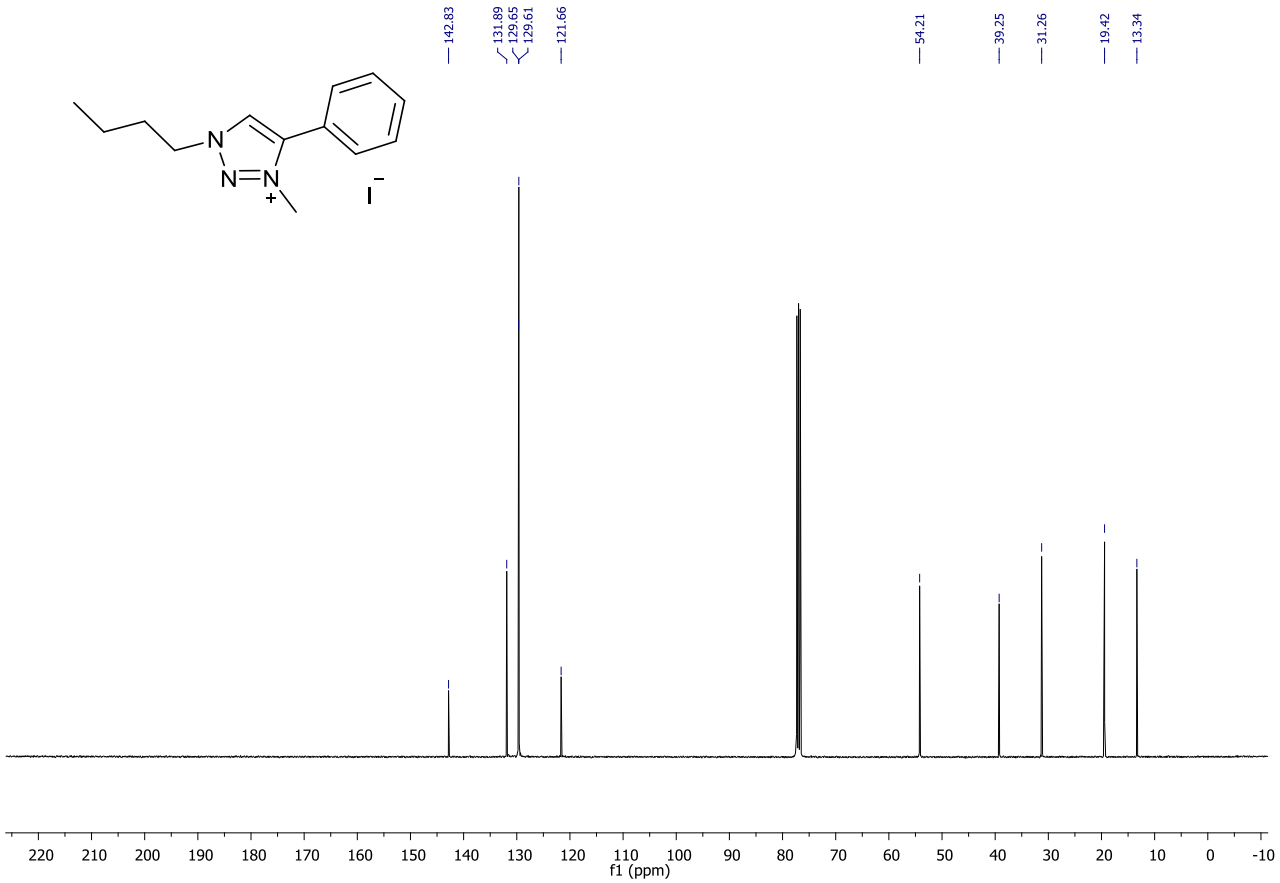

Figure S37. ^{13}C NMR spectra of 1-butyl-3-methyl-4-phenyl-1*H*-1,2,3-triazolium iodide (**2c**)

16. HRMS of complexes 3a-c

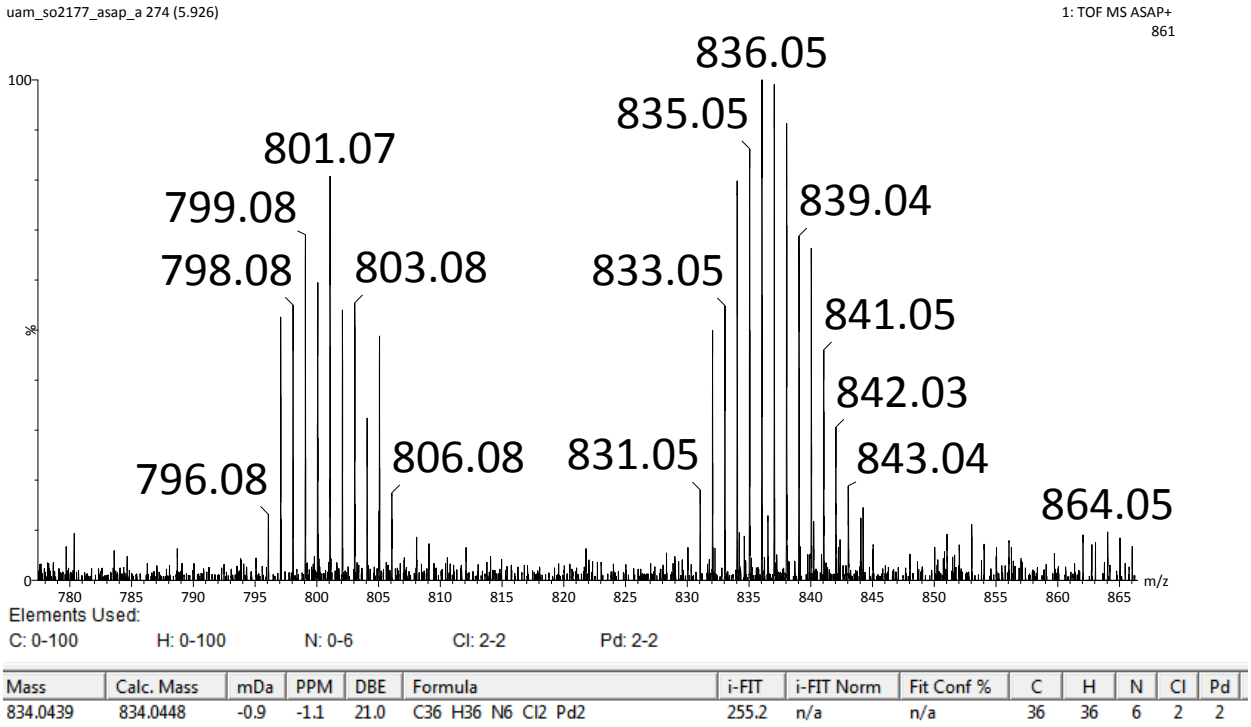

Mass	Calc. Mass	mDa	PPM	DBE	Formula	i-FIT	i-FIT Norm	Fit Conf %	C	H	N	Cl	Pd
834.0439	834.0448	-0.9	-1.1	21.0	C36 H36 N6 Cl2 Pd2	255.2	n/a	n/a	36	36	6	2	2

Figure S38. HRMS of **3a**

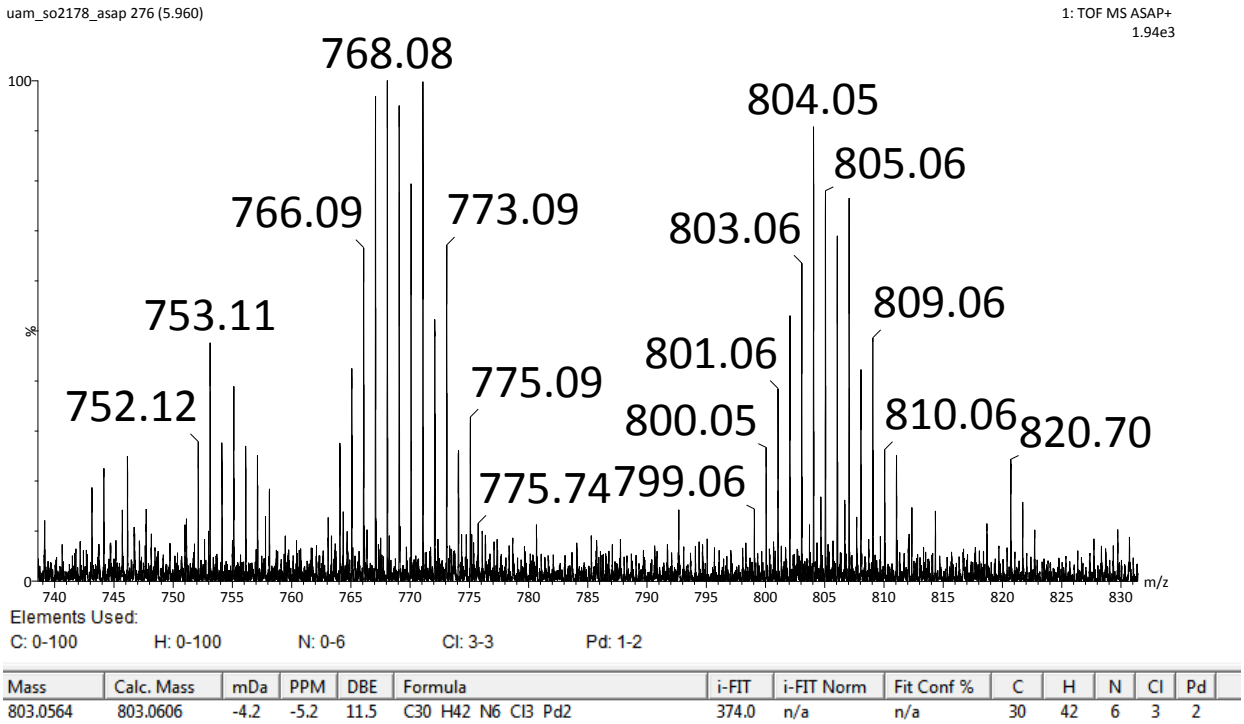

Mass	Calc. Mass	mDa	PPM	DBE	Formula	i-FIT	i-FIT Norm	Fit Conf %	C	H	N	Cl	Pd
803.0564	803.0606	-4.2	-5.2	11.5	C30 H42 N6 Cl3 Pd2	374.0	n/a	n/a	30	42	6	3	2

Figure S39. HRMS of **3b**

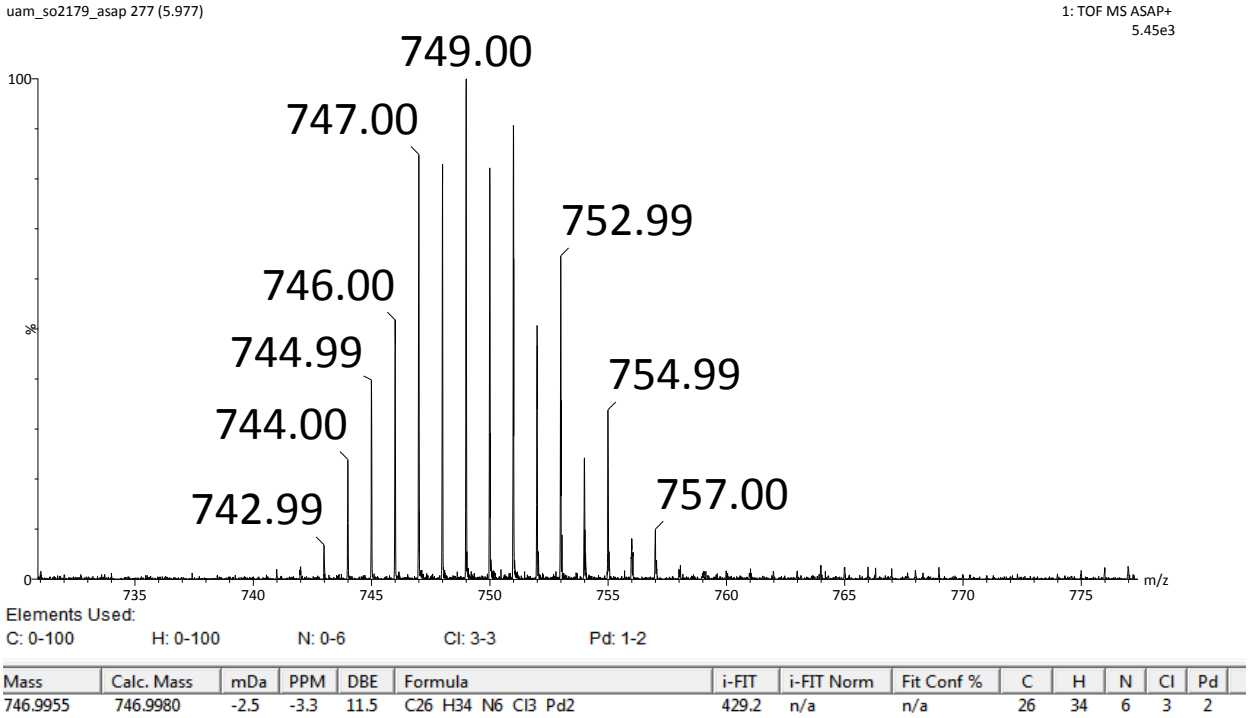

Mass	Calc. Mass	mDa	PPM	DBE	Formula	i-FIT	i-FIT Norm	Fit Conf %	C	H	N	Cl	Pd
746.9955	746.9980	-2.5	-3.3	11.5	C26 H34 N6 Cl3 Pd2	429.2	n/a	n/a	26	34	6	3	2

Figure S40. HRMS of **3c**

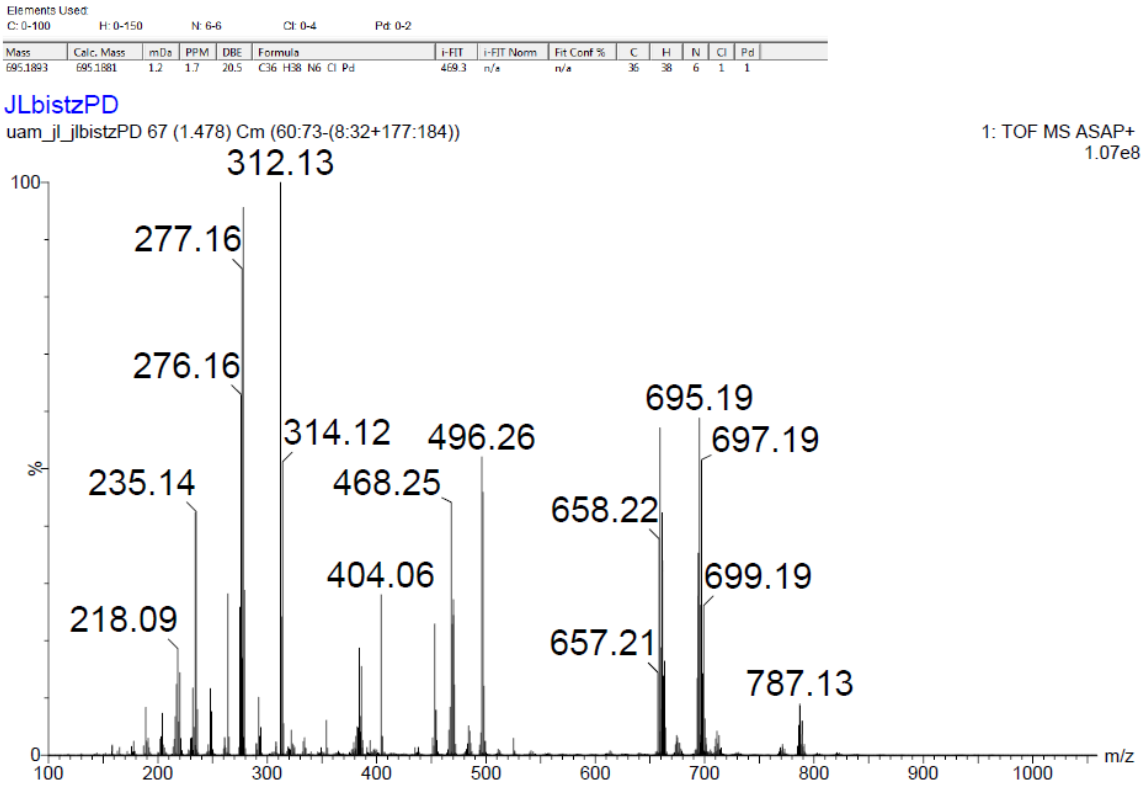

Figure S41. MS and HRMS of **4** (independent synthesis)

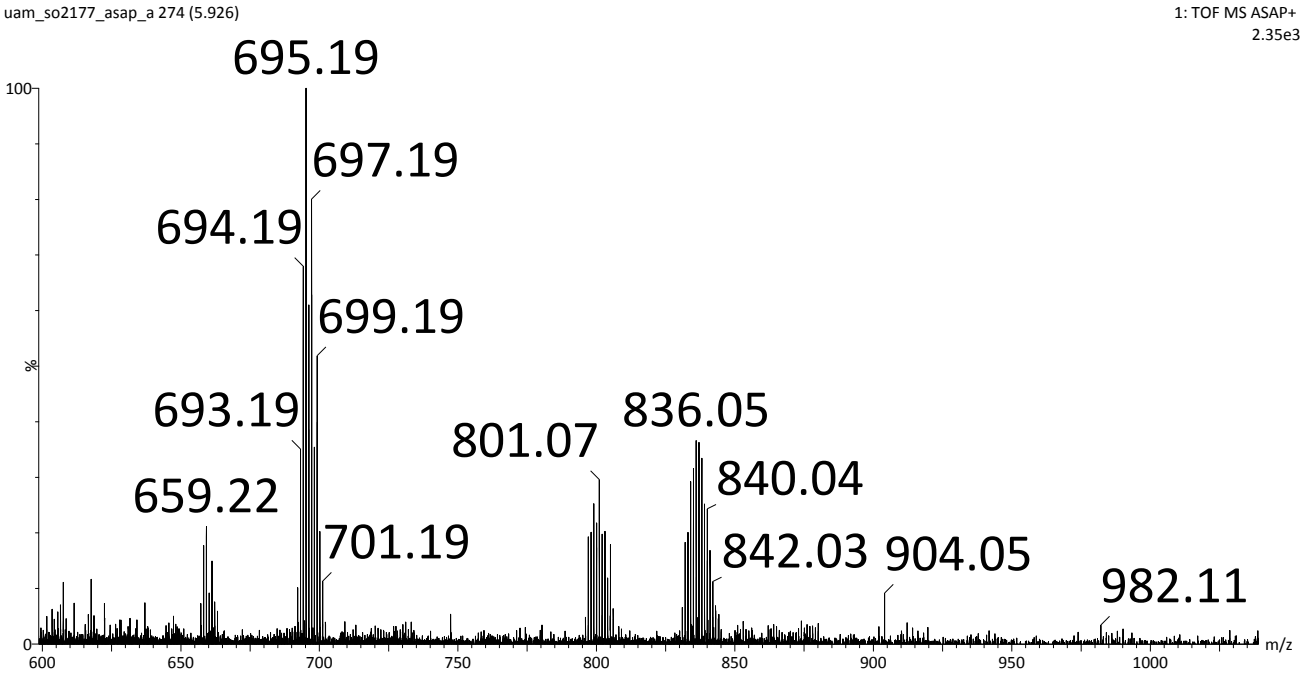

Figure S42. Disproportionation of **3a**. Mass spectrum of the post reaction mixture.

Display Report

Analysis Info

Analysis Name	D:\Data\Gosia\J.Lorkowski\JP 273_17.12.05_1.d				
Method	Tune_pos_Standard.m		Operator	malgorzata kasperkowiak	
Sample Name	JP 273		Instrument	impact HD	1819696.00156
Comment					

Acquisition Parameter

Source Type	ESI	Ion Polarity	Positive	Set Nebulizer	1.0 Bar
Focus	Active	Set Capillary	4000 V	Set Dry Heater	200 °C
Scan Begin	50 m/z	Set End Plate Offset	-500 V	Set Dry Gas	4.0 l/min
Scan End	800 m/z	Set Charging Voltage	2000 V	Set Divert Valve	Source
		Set Corona	0 nA	Set APCI Heater	0 °C

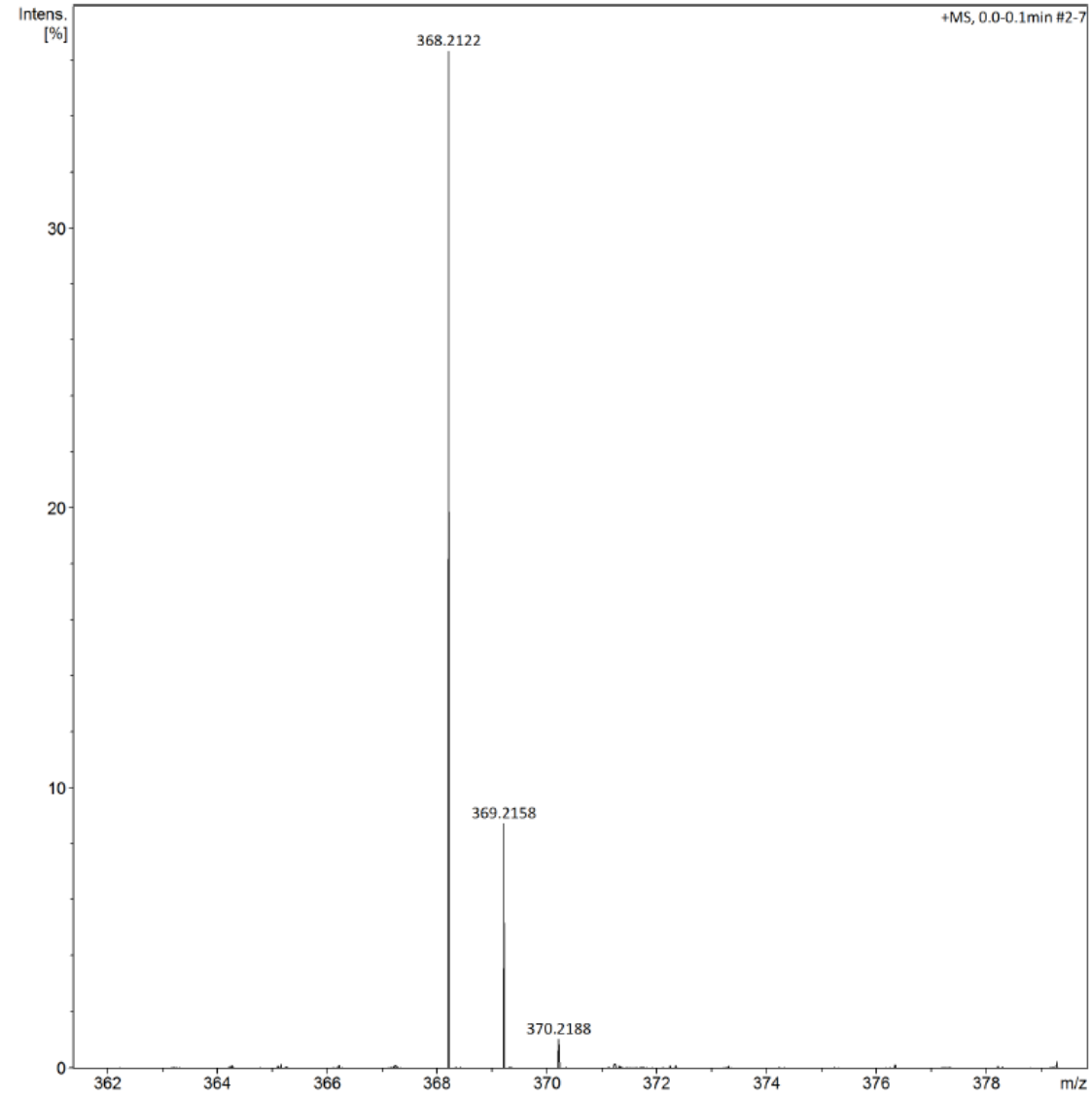

Figure S43. HRMS of **8**

17. References

S1 K. Barral, A. Moorhouse, J. Moses, *Org. Lett.* **2007**, *9*, 1809–1811.

S2 R. Thorwirth, A. Stolle, B. Ondruschka, A. Wild, U. Schubert, *Chem. Commun.* **2011**, *47*, 4370–4372.

S3 K. Kilpin, S.Crot, T. Riedel, J. Kitchen, P. Dyson, *Dalton Trans.* **2014**, *43*, 1443–1448.

S4 A. Poulain, D. Canseco-Gonzalez, R. Hynes-Roche, H. Müller-Bunz, O. Schuster, H. Stoeckli-Evans, A. Neels, M. Albrecht, *Organometallics* **2011**, *30*, 1021–1029.

S5 R. Saravanakumar, V. Ramkumar, S. Sankararaman, *Organometallics* **2011**, *30*, 1689–1694.

S6 D. Canseco-Gonzalez, A. Gniewek, M. Szulmanowicz, H. Müller-Bunz, A. Trzeciak, M. Albrecht, *Chem. Eur. J.* **2012**, *18*, 6055–6062.

S7 H. Nulwala, C. Tang, B. Kail, K. Damodaran, P. Kaur, S. Wickramanayake, W. Shi, D. Luebke, *Green Chem.* **2011**, *13*, 3345–3349.

S8 CrysAlisPro 1.171.38.34a (Rigaku OD, **2015**).

S9 Sheldrick, G. M. *Acta Cryst.* **2014,** *C71*, 3–8.

S10 A. L. Spek, *Acta Cryst.* **2015**, *C71*, 9–18.

S11 A. Gierer and K. Z. Wirtz, *Z. Naturforsch., A: Astrophys. Phys. Phys. Chem*. **1953**, *8*, 532–538.

S12 H.-C. Chen and S.-H. Chen, *J. Phys. Chem*. **1984**, *88*, 5118–5121.

S13 D. Li, G. Kagan, R. Hopson, P. G. Williard, *J Am Chem Soc*. **2009**, *131*, 5627–5634.

S14 Jmol – an open-source Java viewer for chemical structures in 3D. http://www.jmol.org/.

S15 H. Kovacs, A. E. Mark, J. Johansson, W. F. van Gunsteren, *J. Mol. Biol*. **1995**, *247*, 808–822.

S16 N. D. Favera, L. Guènèe, G. bernardelli and C. Piguet, *Dalton Trans.* **2009**, 7625–7638.

S17 M. J. Frisch, G. W. Trucks, H. B. Schlegel, G. E. Scuseria, M. A. Robb, J. R. Cheeseman, G. Scalmani, V. Barone, B. Mennucci, G. A. Petersson, H. Nakatsuji, M. Caricato, X. Li, H. P. Hratchian, A. F. Izmaylov, J. Bloino, G. Zheng, J. L. Sonnenberg, M. Hada, M. Ehara, K. Toyota, R. Fukuda, J. Hasegawa, M. Ishida, T. Nakajima, Y. Honda, O. Kitao, H. Nakai, T. Vreven, J. A. Montgomery Jr., J. E. Peralta, F. Ogliaro, M. Bearpark, J. J. Heyd, E. Brothers, K. N. Kudin, V. N. Staroverov, T. Keith, R. Kobayashi, J. Normand, K. Raghavachari, A. Rendell, J. C. Burant, S. S. Iyengar, J. Tomasi, M. Cossi, N. Rega, J. M. Millam, M. Klene, J. E. Knox, J. B. Cross, V. Bakken, C. Adamo, J. Jaramillo, R. Gomperts, R. E. Stratmann, O. Yazyev, A. J. Austin, R. Cammi, C. Pomelli, J. W. Ochterski, R. L. Martin, K. Morokuma, V. G. Zakrzewski, G. A. Voth, P. Salvador, J. J. Dannenberg, S. Dapprich, A. D. Daniels, O. Farkas, J. B. Foresman, J. V. Ortiz, J. Cioslowski and D. J. Fox, Gaussian 09, Revision B.01, Gaussian, Inc., Wallingford CT, 2010.

S18 A. D. Becke, *J. Chem. Phys*. **1993**, *98*, 5648–5653.

S19 C. Lee, W. Yang and R. G. Parr, *Phys. Rev. B: Condens. Matter*, 1988, **37**, 785–789.